



Review

iPSC-Derived Cardiomyocytes in Inherited Cardiac Arrhythmias: Pathomechanistic Discovery and Drug Development

Eline Simons , Bart Loeys and Maaïke Alaerts *

Cardiogenetics Research Group, Center of Medical Genetics, University of Antwerp and Antwerp University Hospital, 2650 Antwerp, Belgium

* Correspondence: maaïke.alaerts@uantwerpen.be

Abstract: With the discovery of induced pluripotent stem cell (iPSCs) a wide range of cell types, including iPSC-derived cardiomyocytes (iPSC-CM), can now be generated from an unlimited source of somatic cells. These iPSC-CM are used for different purposes such as disease modelling, drug discovery, cardiotoxicity testing and personalised medicine. The 2D iPSC-CM models have shown promising results, but they are known to be more immature compared to in vivo adult cardiomyocytes. Novel approaches to create 3D models with the possible addition of other (cardiac) cell types are being developed. This will not only improve the maturity of the cells, but also leads to more physiologically relevant models that more closely resemble the human heart. In this review, we focus on the progress in the modelling of inherited cardiac arrhythmias in both 2D and 3D and on the use of these models in therapy development and drug testing.

Keywords: iPSC; cardiac arrhythmia; iPSC-derived cardiomyocytes



Citation: Simons, E.; Loeys, B.; Alaerts, M. iPSC-Derived Cardiomyocytes in Inherited Cardiac Arrhythmias: Pathomechanistic Discovery and Drug Development. *Biomedicines* **2023**, *11*, 334. <https://doi.org/10.3390/biomedicines11020334>

Academic Editor: M. Esther Gallardo

Received: 25 December 2022

Revised: 20 January 2023

Accepted: 22 January 2023

Published: 25 January 2023



Copyright: © 2023 by the authors. Licensee MDPI, Basel, Switzerland. This article is an open access article distributed under the terms and conditions of the Creative Commons Attribution (CC BY) license (<https://creativecommons.org/licenses/by/4.0/>).

1. Introduction

Since the discovery of induced pluripotent stem cells (iPSCs) in 2006 by Takahashi and Yamanaka [1], iPSCs have increasingly gained popularity in the scientific field; not only to perform stem cell research but also to create somatic cells derived from these iPSCs such as neurons [2], cardiomyocytes [3] and hepatic cells [4] amongst many others. The numerous advantages, such as access to difficult-to-access human cell types, the development of patient-specific cell types, decreased need for laboratory animals and less ethical concerns compared to embryonal stem cells (ESC), are well-known. However, there are also some drawbacks on the use of these derived cells such as variability, low differentiation efficiency and the immature state of the differentiated cells. Nevertheless, iPSC-derived cells are indispensable in the current cell-biology research community.

In 2009, Zwi et al. presented their work on the development of a way to differentiate iPSCs into cardiomyocytes [3]. Their iPSC-derived cardiomyocytes (iPSC-CM) expressed the cardiac specific markers cardiac troponin-I and sarcomeric α -actinin, were electrophysiologically active and they displayed the expected response to the admission of different drugs. Ever since, an increasing number of papers have been published using iPSC-CM to model diseases, perform drug and cardiotoxicity testing and develop new therapies.

In this review, we take a closer look at these recent developments focusing on cardiac arrhythmia disorders and the transition from 2D to 3D culture models (Figure 1).

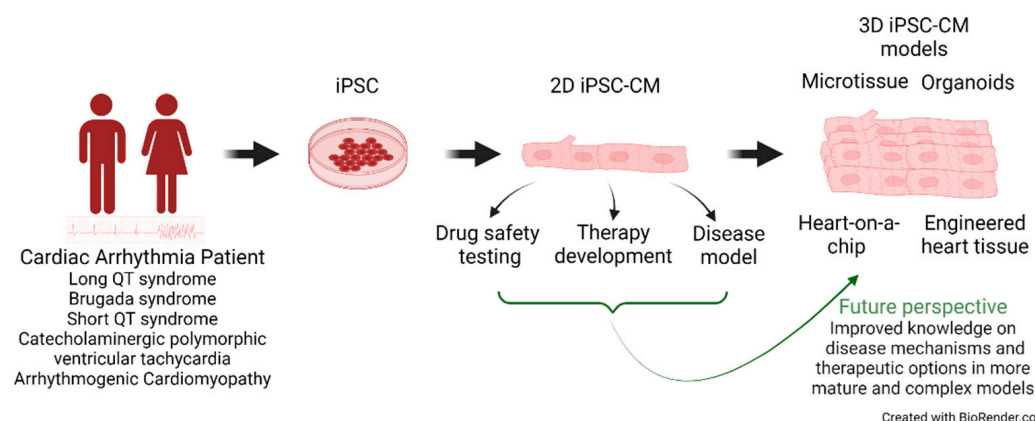


Figure 1. Schematic representation of different applications of iPSC-cardiomyocytes.

2. iPSC-Derived Cardiomyocytes as Inherited Cardiac Arrhythmia Models

Inherited cardiac arrhythmias are characterised by the dysfunction of cardiac ion channels, their accessory proteins or cell–cell contact proteins which can lead to ventricular arrhythmias and potential sudden cardiac death. The most well-known inherited cardiac arrhythmias include long QT syndrome (LQTS), Brugada syndrome (BrS), catecholaminergic polymorphic ventricular tachycardia (CPVT), short QT syndrome (SQTS) and arrhythmogenic cardiomyopathy (ACM). These diseases are caused by pathogenic variants in genes encoding components or accessory elements of these ion channels or desmosomes. The type of mutation (loss-of-function (LOF) or gain-of-function (GOF)) is also important in defining the disease outcome.

The arrhythmias mostly occur in the ventricles, making ventricular cardiomyocytes the most relevant cell type to investigate. Most of the currently used iPSC-CM differentiation protocols generate a mixture of atrial, ventricular and sinoatrial pacemaker cardiomyocytes, but with a clear overrepresentation/higher presence of ventricular cells. Ventricular action potentials (AP) are characterised by a more negative maximum diastolic potential, a rapid AP upstroke, a long plateau phase and an APD90/APD50 ratio $\leq 1.3/1.4$ [5–7]. It is also possible to differentiate iPSCs directly into the specific cardiomyocyte types [8].

In 2018, Garg et al. reviewed the published iPSC-CM models of several channelopathies [9] and Pan et al. updated this review with the addition of ACM (Table S1 (Supplementary Materials)) [10]. Here, the overview is updated (see Table 1) with more recently published models.

Table 1. Overview of published 2D iPSC-CM cardiac arrhythmia disease models.

Syndrome	Causal Gene Variant	Experimental Approach	Cellular Phenotype	Ref.
LQTS	<i>KCNQ1</i> p.(Arg190Gln)	PC, IF	Prolonged AP, reduced I_{Ks} current, ER retention, increased susceptibility to catecholamine-induced tachyarrhythmia, attenuation of this phenotype with beta blockade	[6]
	<i>KCNH2</i> p.(Thr983Ile)	PC, MEA, WB, CI	Prolonged APD50 and APD90, beat irregularity, EAD, decreased I_{Kr} density, reduced channel surface expression, higher diastolic Ca^{2+}	[11]
	<i>CACNA1C</i> p.(Asn639Thr)	CardioExcyte 96, PC	Prolonged Maximum Field Potential Duration and APD, slower $Ca_v1.2$ voltage-dependent inactivation	[12]
BrS/LQT	<i>SCN5A</i> p.(1798insAsp)	PC	Reduced I_{Na} peak current, persistent I_{Na} , reduced V_{max} , prolonged APD90	[13]

Table 1. Cont.

Syndrome	Causal Gene Variant	Experimental Approach	Cellular Phenotype	Ref.
BrS	SCN5A p.(Arg620His)+ p.(Arg811His) SCN5A (c. 4190delA)	PC, CI	Reductions in I_{Na} and V_{max} of AP, increased burden of triggered activity, abnormal calcium transients and beating interval variation	[14]
	CACNB2 p.(Ser142Phe)	PC, CI	Reduction in peak I_{Ca-L} , acceleration recovery of inactivation and altered voltage dependent inactivation, reduced APA and V_{max} , reduced protein expression of the CACNB2 gene, increased arrhythmia-like events, suppression of arrhythmic events by quinidine and bisoprolol	[15]
	SCN5A p.(Val1405Met) SCNB1 p.(Ala197Val)	PC, CI	Reduction in peak I_{Na} density, reduced APA and V_{max} , prolonged AP, more proarrhythmic events (EAD, DAD-like events), reduced Nav1.5 protein expression	[16]
	SCN5A p.(Ser1812X)	PC, IF, MEA	Reduced I_{Na} and a delayed sodium channel activation, slowed AP upstroke velocity, reduced FP and CV, enhanced I_{to} and an augmented I_{Ca-L} window current, reduced Nav1.5 protein expression	[17]
SQTS	KCNH2 p.(Asn588Lys)	PC, IF, CI	Shortening APD, Increased I_{Kr} tail current, arrhythmic events, increased hERG expression, re-entrant arrhythmias	[18,19]
	KCNH2 p.(Thr618Ile)	PC, WB	Increased I_{kr} , shortened APD, beat-to-beat variability, increased membrane expression	[20]
CPVT	RYR2 p.(Phe2483Ileu)	PC, MEA, CI	Arrhythmias, DAD, forskolin can rescue these phenotypes	[21]
	RYR2 p.(Phe2483Ile)	CI	Longer Ca^{2+} sparks, higher diastolic Ca^{2+} levels, irregular beating, SR calcium leak and lower load levels	[22]
	RYR2 p.(Asp3638Ala)	AFM, CI, PC,	Higher beat rate, diastolic SR Ca^{2+} leak, weaker force contraction during stress, APD, V_{max} and APA decreased during stress	[23]
	RYR2 p.(Arg176Gln)	CI	Aberrant diastolic SR Ca^{2+} release, EAD	[24]
	RYR2 p.(Gln4201Arg) p.(Arg420Gln) p.(Phe2483Ile)	PC, CI, qPCR, WB	p.(Gln4201Arg): decrease mRNA levels RYR2, protein similar, All mutants: longer sparks p.(Arg420Gln): lower spark frequency	[25]
	RYR2 p.(Phe13Leu) p.(Leu14Pro) p.(Arg15Pro) p.(Arg176Gln)	CI, WB, qPCR, MEA LEAP	Increased Ca^{2+} amplitude and upstroke velocity, decrease in calcium transient duration, irregular beating, decreased beat rate	[26]
	CASQ2 p.(Asp307His)	PC, CI, EM	DADs, oscillatory arrhythmic, after-contractions and diastolic $[Ca^{2+}]_i$ rise, less organised myofibrils, enlarged SR cisternae and reduced number of caveolae	[27]

Table 1. Cont.

Syndrome	Causal Gene Variant	Experimental Approach	Cellular Phenotype	Ref.
ACM	<i>PKP2</i> p.(Leu614Pro)	PC, CI, qPCR, IF	Reduction in rate of spontaneous cell contraction and amplitude under nifedipine, reduced expression plakophilin2 and plakoglobin	[28]
	<i>DSG2</i> p.(Gly638Arg)	IF, PC, CI, qPCR	Lower APA and Vmax, decreased peak I_{Na} , I_{NCX} , I_{to} , I_{SK} , and I_{KATP} , increased I_{Kr} , more arrhythmogenic events	[29]
	<i>DSG2</i> p.(Gly638Arg)	PC, WB, qPCR	Upregulation of SK4 and NDPK-B, enhanced SK4 channel currents, pacemaker activity and more arrhythmic events	[30]

Adapted and updated from Garg et al. (2018) and Pan et al. (2021) [9,10]. PC: patch clamp; IF: immunofluorescence; MEA: Multi electrode array; WB: Western Blot; CI: Calcium imaging; AFM: atomic force microscopy; AP: action potential; I_{Ks} : slow delayed rectifier K⁺ current; ER: endoplasmic reticulum; APD50-90: Action potential duration at 50–90% of repolarisation; EAD: early after depolarisation; I_{Kr} : rapid delayed rectifier K⁺ current; I_{Ca-L} : L-type calcium current; APA: action potential amplitude; Vmax: maximum rate of rise of the action potential; I_{Na} : sodium current; DAD: delayed after repolarisation; FP: field potential; CV: conduction velocity; I_{to} : transient outward current; SR: sarcoplasmic reticulum; EM: electron microscope.

2.1. Long QT Syndrome

Long QT syndrome has a prevalence of 1 in 2000 and is clinically diagnosed by a prolongation of the QT interval (heart rate-corrected QT interval ≥ 480 ms) on the electrocardiogram (ECG) [31]. Currently, there are 17 subtypes of LQTS based on the gene involved and the most common subtypes are LQT1, LQT2 and LQT3, caused by mutations in the *KCNQ1*, *KCNH2* and *SCN5A* genes, respectively [32]. Over the years, several LQTS iPSC-CM models have been published, the first in 2010 by Moretti et al. [6]. The latter investigated patient-specific iPSC-CM of three related LQT1 patients harbouring a p.(Arg190Gln) variant and showed a prolonged action potential duration at 90% of repolarisation (APD90) and lower potassium current densities compared to control individuals. This corresponded to the phenotype observed in the patients. Since then, several papers have been published describing LQTS iPSC-CM models of known pathogenic mutations (reviewed by Garg et al. [9], Table S1). More recently, LQTS iPSC-CM models have been used to investigate the pathogenicity of variants of uncertain significance (VUS). For example, Garg et al. created a LQT2 iPSC-CM model harbouring the VUS p.(Thr983Ile) in the *KCNH2* gene. Using CRISPR/Cas9 technology, they developed both a homozygous VUS cell line as well as an isogenic control line. Both patch-clamp and multi-electrode array (MEA) experiments showed prolonged APD50, APD90 and field potential duration (FPD) in the homozygous as well as in the heterozygous VUS iPSC-CMs. In addition, more beat irregularity or early after depolarisations (EADs) were observed and the phenotype of the homozygous VUS iPSC-CMs resembled that of the known pathogenic p.(Ala561Val) *KCNH2* variant. Potassium (I_{Kr}) current was decreased in the VUS cell line and restored to normal current densities in the isogenic control [11]. Chavali et al. took a different CRISPR/Cas9 approach when they introduced a VUS p.(Asn639Thr) in the *CACNA1C* gene into iPSCs to create a patient-independent iPSC model. Prolonged APD and FPD were recorded due to a slower inactivation of the $Ca_v1.2$ current. As this cellular phenotype recapitulated the patient phenotype, the authors reclassified the VUS as probably pathogenic [12].

2.2. Brugada Syndrome

Brugada syndrome is a cardiac arrhythmia with a prevalence ranging from 1 in 500 to 1 in 2000 and patients display a specific ST-segment elevation on the ECG. Many genes encoding ion channels and accessory proteins have been associated with the disease but only one is currently considered as causal, namely *SCN5A*, encoding the cardiac sodium channel $Na_v1.5$. Mutations in *SCN5A* account for up to 20–25% of the BrS cases [33,34]. The first report on iPSC-CM in BrS was published by Davis et al. They modelled an iPSC-

CM line harbouring a *SCN5A* mutation p.(1798insAsp) from a patient with an overlap syndrome of LQT/BrS and conduction disorder. Reduced and persistent sodium currents, slower upstroke velocity and prolongation of APD90 were observed in patients' iPSC-CMs but not in controls, mimicking the LOF and GOF phenotype of this mutation [13]. Later, two iPSC-CM lines from BrS patients with *SCN5A* (p.(Arg620His)+ p.(Arg811His) and c.4190delA) mutation were evaluated by Liang et al. Both cell lines showed abnormal action potentials (AP) compared to the controls as well as a reduced sodium current [14]. In 2021, Nijak et al. published a review on iPSC-CM models generated of BrS patients, included in Table S1 [35]. More recently, extra reports on BrS iPSC-CM models harbouring variants in *SCN5A* (p.(Val1405Met), p.(Ser1812X)), *SCN1B* (p.(Ala197Val)) and *CACNB2* (p.(Ser142Phe)) were published. Reduced expression of the encoded proteins was observed as well as reduced sodium or calcium currents leading to reduced action potential amplitude (APA) and maximum upstroke velocity (V_{max}) but prolonged APDs [15–17]. Calcium imaging showed more proarrhythmic events such as EADs and DADs (early and delayed after depolarisations) in BrS cell lines compared to control cell lines [16]. A *SCN5A* p.(Ser1812X) variant resulted in reduced conduction velocity and proarrhythmic events [17].

2.3. Short QT Syndrome

Short QT syndrome is diagnosed by a shortening of the QT interval on the ECG and has a prevalence ranging from 1 in 1000 to 1 in 5000 [36]. Causal GOF mutations are mostly found in potassium channel genes such as *KCNH2*, *KCNQ1* and *KCNJ2* [37]. The first iPSC-CM model of SQTs was published by El-Battrawy et al. in 2018 where one patient cell line with a p.(Asn588Lys) mutation in the *KCNH2* gene was compared to two control cell lines. They demonstrated an upregulation of the hERG channel expression and increased potassium currents (I_{Kr}) resulting in a shortening of the action potential. During calcium-handling experiments, irregular beating, DAD-like and EAD-like arrhythmic events were recorded more in patient iPSC-CMs compared to control iPSC-CMs [18]. Later, the same mutation and another *KCNH2* p.(Thr618Ile) variant were modelled in iPSC-CMs and similar electrophysiological and molecular results were obtained [19,20]. An iPSC-based cardiac cell sheet model was created by Shinnawi and colleagues and an increase in susceptibility to the development of re-entrant arrhythmias recorded [19]. The p.(Thr618Ile) variant did not give rise to any arrhythmic events. However, there was an increased beat-to-beat variability in the patient cell line [20].

2.4. Catecholaminergic Polymorphic Ventricular Tachycardia Type

CPVT most often occurs in young adults and athletes and is triggered by β -adrenergic stimulation related to exercise or emotional stress. It is mainly caused by mutations in Ca^{2+} -handling related genes such as *RYR2* and *CASQ2* and has an estimated prevalence of 1 in 10,000 [37,38]. Both proteins are essential in the Ca^{2+} handling in heart and muscle cells, responsible for the proper contraction of the cells. Different iPSC-CM CPVT models have been developed (reviewed by Garg et al. in 2018 [9], included in Table S1). The first CPVT iPSC-CM model from a patient carrying a *RYR2* pathogenic variant (p.Phe2483Ile) was published in 2011 by Fatima et al. The analysis revealed more DAD events in patient iPSC-CMs compared to control iPSC-CMs and embryonal stem cell-derived cardiomyocytes (ESC-CM), recapitulating the CPVT phenotype. The underlying aberrant sarcoplasmic reticulum (SR) Ca^{2+} release in the iPSC-CMs is responsible for the development of these DADs and arrhythmias [21]. The same variant was modelled using CRISPR/Cas9 by Wei et al. and showed longer calcium sparks in both hetero- and homozygous iPSC-CMs, larger SR Ca^{2+} leak levels and smaller load levels which is consistent with higher diastolic Ca^{2+} levels [22]. In 2018, Acimovic et al. published an iPSC-CM model of a CPVT patient with a *RYR2* p.(Asp3638Ala) variant. They found an increase in beat rate in the patient cell line compared to both iPSC- and ESC-derived CMs and a weaker response in force contraction upon stress induction. Calcium handling was normal under basal conditions, but upon stress more irregular Ca^{2+} -release events in CPVT iPSC-CMs were

recorded. Patch clamp data revealed a prolongation of the AP in basal conditions while during stress, APD, V_{max} and the amplitude were lower in CPVT CMs compared to controls [23]. Several other reports on *RYR2* variants, either from patient-specific [24,26] or CRISPR/Cas9-induced iPSC-CMs [25], show similar aberrant Ca^{2+} handling although mutant lines also differ from each other, for example in the magnitude of the Ca^{2+} leak or SR Ca^{2+} content [24–26]. Two *CASQ2* (p.(Asp307His)) patient-specific iPSC-CM models showed DADs, oscillatory prepotentials, after-contractions and diastolic $[Ca^{2+}]_i$ rises similar to *RYR2* CPVT models [27].

2.5. Arrhythmogenic Cardiomyopathy

ACM, previously known as arrhythmogenic right ventricular cardiomyopathy (ARVC), is a rare disease (1 in 5000) that is characterised by fibrofatty myocardial replacement, leading to impaired ventricular systolic function and ventricular arrhythmias. Mutations in desmosomal genes such as *PKP2*, *DSG2*, *DSP*, *DSC2* and *JUP* play a prominent role in the development of the disease [39]. The first model of ARVC was published in 2013 by Ma et al. They created a patient-specific iPSC-CM model with a *PKP2* p.(Leu614Pro) mutation and showed downregulation of the expression of plakophilin and plakoglobin but no other desmosomal genes [28]. El-Battrawy and Buljubasic studied the same patient-derived iPSC-CM ACM model harbouring a mutation in the *DSG2* gene (p.(Gly638Arg)) [29,30]. The amplitude and the upstroke velocity of the AP were decreased as well as peak I_{Na} , I_{NCX} , I_{to} , I_{SK} and I_{KATP} , while I_{Kr} on the contrary was enhanced. Mutant iPSC-CMs showed more arrhythmogenic effects compared to control cells [29]. In addition, Buljubasic further investigated the underlying molecular mechanisms and revealed upregulation of SK4 channels and NDPK-B resulting in increased I_{SK4} , pacemaker activity and arrhythmic events [30].

3. From 2D to 3D

In the iPSC-CM field, immaturity of the created iPSC-CM is a well-known problem. As the cardiomyocytes often only stay in culture for 30 days or less, it is not surprising that the phenotype of these cells does not fully recapitulate the phenotype of a mature native cardiomyocyte that has been developing for many years. Ahmed et al. (2020) reviewed the currently applied methods of maturation and pinpointed the main differences between fetal-like iPSC-CMs and adult cardiomyocytes. Methods to promote maturation include prolonged culture, addition of hormones (e.g., thyroid hormone) or cellular energy source (e.g., fatty acids such as palmitate, oleic acid, linoleic acid), co-culture, extracellular matrix, mechanical or electrical stimulation and 3D culture [40]. The latter is not only beneficial for the maturity of the cardiomyocytes but also enables the creation of 3D models that are more similar to native heart tissue. The heart consists of cardiomyocytes, but also various other cell types are present in the tissue such as endothelial cells (EC), fibroblasts (FB), pericytes, smooth muscle cells, immune cells (myeloid and lymphoid), adipocytes, mesothelial cells and neuronal cells [41]. Meanwhile, Pinto et al. found that CMs accounted for only 25–35% of the cells in the heart, ECs for 60% and FBs for less than 20%; Litviňuková found CMs represented 30% to 50% of the cells in atrial and ventricular samples, respectively, while ECs represented 10% and FBs 20% [41,42]. Adding these extra cell types to the model will make it even more physiologically relevant and likely more suitable for modelling pathological conditions and downstream applications such as drug or cardiotoxicity screening.

Below, we will discuss the development from 2D to 3D iPSC-CM cultures with or without other cell types using scaffold-free and scaffold-based techniques.

3.1. Scaffold-Free 3D Culture

One method to create a 3D cell culture is the scaffold-free hanging droplet method in which iPSC-CMs are placed in a droplet in an ultra-low attachment plate with [43,44] or without [45,46] the addition of other cell types such as cardiac fibroblasts and endothelial cells. Beauchamp et al. and Ergir et al. reported a long-term stable 3D model of iPSC-CMs

that was able to respond to electrical, pharmacological, and physical stimuli but Ca^{2+} dyes only partially penetrated the culture and the CMs still displayed more fetal-like features such as shorter sarcomeres [45,46]. Sharma et al. combined iPSC-CM with human cardiac fibroblasts (HCFs) and human coronary artery endothelial cells to create cardiac spheroids containing a cardiac endothelial cell network that recapitulated better than the in vivo human heart [44].

Organoids are mainly formed by differentiating iPSC directly to CM (and other cell types) in ultra-low attachment plates. Drakhlis et al. generated a model of heart-forming organoids (HFO) by differentiating free-floating iPSC aggregates into cardiac organoids that resemble the early embryonic heart as they are composed of a myocardial layer and endocardial-like cells. They were able to model a *NKX2.5* KO which resulted in similar cardiac malformations such as decreased cardiomyocyte adhesion and hypertrophy as observed in in vivo mouse studies [47]. A similar HFO protocol by Lewis-Israeli et al. using different small molecules' concentrations and adding one WNT pathway modulation step enabled the generation of multiple cardiac-specific cell lineages such as endo- and epicardial cells, endothelial cells and cardiac fibroblasts [48]. Lee et al. started from embryonic bodies and generated chamber-forming HFOs. RNA-seq revealed that they more closely resembled the fetal heart than adult heart tissue, but here as well, several cell types were generated [49]. As such, a drawback of this technique is that the iPSC-CMs still display an immature phenotype but the HFOs are well suited to studying cardiac diseases linked to development.

Another scaffold-free method is used to create cardiac microtissues (cMT) where several (previously generated) cell types (CMs, ECs, FBs, . . .) are combined. Giacomelli et al. combined iPSC-derived ECs, iPSC-derived cardiac FBs and iPSC-CMs to form a micro-tissue displaying mature iPSC-CM ultrastructures such as elongated tubular myofibrils and T-tubule-like structures [50]. RNA-seq indicated a mature expression profile of the iPSC-CMs comparable to that of adult CMs. Electrophysiological maturation was proven by the presence of the typical AP notch, although this has also been observed in 2D cultures [17,51]. As a proof-of-concept they created a cMT consisting of healthy iPSC-CMs and iPSC-ECs combined with mutant cardiac FB of an ACM patient with a *PKP2* (c.2013delC, p.(Lys672ArgfsX12)) mutation (Table 2) and found reduced Cx43 expression in ACM cMT as well as arrhythmic behaviour [50], highlighting the importance of the presence of these non-myocytes in the model. In another paper, a LQTS cMT harbouring a *KCNQ1* p.(Arg594Gln) variant, showed a prolonged field potential compared to wild-type cMT [52] proving that the cMT can recapitulate the disease phenotype (Table 2). However, as 2D models already showed this phenotype, the MT model was not of specific added value in this case.

Table 2. Overview of published 3D iPSC-CM arrhythmia models.

3D Model	Disease/Gene/ Variant	Cellular Phenotype	Ref.
Cardiac Microtissue	ACM <i>PKP2</i> (c.2013delC, p.(Lys672ArgfsX12))	Lower Cx43 expression and arrhythmic behaviour of ACM cMT consisting of control CM and EC and ACM cardiac fibroblasts	[50]
Cardiac Microtissue	LQTS <i>KCNQ1</i> p.(Arg594Gln)	Prolonged field potential duration (FPD), β -adrenergic stimulation shortened the RR interval and decreased the FPD	[52]
Engineered heart tissue	LQTS <i>KCNH2</i> p.(Ala614Val)	APD prolongation (via ArcLight), re-entrant arrhythmic activity after I_{Kr} blocking with dofetilide	[53]
Engineered heart tissue	CPVT <i>CASQ2</i> p.(Asp307His)	More $[\text{Ca}^{2+}]_i$ transient abnormalities and arrhythmias compared to control EHT but less than single cell CPVT iPSC-CM	[53]

3.2. Scaffold-Based 3D Culture

Another frequently used method is scaffold-based culture. These scaffolds consist of (decellularised) extracellular matrix (ECM) [54], natural or synthetic polymers [55,56] and can be combined as a hydrogel in an organised well-defined shape or in certain orientations [57]. Fong et al. tested the effect of adult and fetal extracellular matrix from decellularised bovine adult and fetal heart tissue on the maturity of the CMs in both 2D and 3D cultures. Adult heart ECM improved maturation, demonstrated by increased expression of several calcium-handling genes and enhanced calcium signalling, both in 2D and 3D culture with the highest expression levels observed in 3D cultured iPSC-CMs. However, there was no improvement on the formation of T-tubules [54].

In engineered heart tissue (EHT) iPSC-CMs are grown on hydrogel scaffolds wrapped around two flexible pillars that have the ability to mechanically stimulate the cells and improve maturation. Several published models indeed prove that CMs grown in EHT present more mature electrophysiological properties such as action potential amplitude and upstroke velocity and more mature rod-shape morphology and sarcomere alignment [58]. Expression profiles as well as the cardiac ultrastructure, bioenergetics and t-tubule formation of stimulated EHT are more in line with adult cardiac tissue than fetal cardiac tissue [59]. To improve maturation even more, Lu et al. induced progressive stretch on the EHT which led to higher contractility and passive elasticity, more mature excitation/contraction coupling and a higher ratio of beta-myosin heavy chain (MHC) by alpha-MHC mRNA [60]. Goldfracht et al. combined the use of ECM with EHT, and in comparison, using a 2D model they found an increased expression of cardiac-related genes and the cardiomyocytes were arranged anisotropically and developed relatively elongated and oriented cell alignments. They created a LQTS2 (*KCNH2* p.(Ala614Val)) and CPVT2 (*CASQ2* p.(Asp307His)) (Table 2) model and using voltage and calcium dyes, AP prolongation in LQTS iPSC-CM was revealed while the CPVT cell model showed abnormal calcium transients and more arrhythmias under stress conditions, indicating that these EHT models can be used to study channelopathies. In comparison with a 2D single cell model, the EHT showed less frequent, severe or complicated arrhythmogenic activity which is clinically more relevant as the extremely high incidence of arrhythmias as recorded in a single cell model would probably be incompatible with life. Re-entrant arrhythmias were not observed at baseline in the LQT-EHT but they were developed after blocking the I_{Kr} , mimicking the clinical situation in LQT patients challenged with a QT prolonging agent [53]. The major advantage of this technique is the maturation state of the CMs, but special equipment for the generation of this EHT is needed, which might not be available for every lab.

3.3. Heart-on-a-Chip

Heart-on-a-chip is a method to culture iPSC-CM—with or without other cell types—in a 2D or 3D manner on a microfluidic device in a chamber with built-in channels for fluids, microactuators and microsensors [61]. Microactuators can give either electrical or mechanical stimuli to the cells/tissue, while the sensors record electrophysiological signals or contraction force [61]. Heart-on-a-chip has been used for drug toxicity assessments and maturation was shown to be improved through electrical and mechanical stimulation [62]. Although some cardiac disease models such as ischaemia and fibrosis have been investigated using the heart-on-a-chip method [63,64], to date there are no publications on its use for inherited cardiac arrhythmias. The technique is currently still under development and the primary focus is on its application for drug cardiotoxicity screening. Even for this application, there are some challenges such as standardisation, reliable tissue manufacturing, high throughput, high content functional readouts and high cost, that still need to be solved before heart-on-a-chip can be more widely used [65,66].

4. Drug and Gene Therapy Testing

4.1. Cardiotoxicity Screening

A first application of iPSC-CMs and their ability to model/display/show arrhythmias and structural pathology is testing of the cardiotoxicity of a drug under development. Cardiotoxicity and arrhythmia induction such as life-threatening Torsade de pointes (TdP) are a main reason for preclinical and clinical drug failure and withdrawal from the market. In 2013, the Comprehensive in Vitro Proarrhythmia Assay (CiPA) initiative was founded to overcome the low specificity of the preclinical studies and clinical trials at that time [67]. One of the novel components is testing the effect of a drug in vitro in iPSC-CM. A total of 28 compounds with known cardiac effects were tested in commercially available iPSC-CMs using a MEA system and voltage-sensitive dyes and could be classified as high-, intermediate- and low-risk for TdP [68]. To confirm these findings, these drugs were tested over several laboratories/facilities, commercial cardiomyocyte types and different MEA platforms and reproducible concentration-dependent electrophysiological responses were reported, indicating that iPSC-CMs can predict clinical QT prolongation and/or arrhythmogenic potential of drug compounds [69–71]. Lee et al. showed that addition of a contractility assay (impedance measurement) into the evaluation of cardiotoxicity provides/allows more mechanistic insights on the drug effect [72]. As discussed above, 3D heart-on-a-chip models are also being tested, holding promise for even better prediction of cardiotoxic and pro-arrhythmic drug effects as they better recapitulated the clinical effects compared to 2D iPSC-CM models as they present occasionally with arrhythmias that are not reported in adult cardiomyocytes [73,74]. Regarding inherited cardiac arrhythmias, variable expressivity is a known characteristic, with many individuals who carry pathogenic variants remaining asymptomatic throughout life. However, specific drugs can also elicit life-threatening arrhythmias in these carriers/patients and patients are recommended to avoid taking them. Using iPSC-CM with such pathogenic variants in cardiotoxicity screening could be a valuable option to predict these adverse effects in a subset of the population.

4.2. Drug Testing

In addition to cardiotoxicity, iPSC-CM can also be deployed to test compounds that could (partially) restore the phenotype of inherited cardiac arrhythmias models (Table 3). Two recent publications reported a 2D LQT3 (*SCN5A* p.(Phe1473Cys)) model that was used to test mexiletine and different analogues in their ability to reduce the prolongation of the AP and they found that the analogues were more potent and selective in inhibiting the late sodium current, responsible for the APD prolongation in patients. In addition, they did not induce AP prolongation or EADs, known off-target effects of mexiletine due to unwanted inhibition of hERG [75], and were still able to suppress arrhythmias [76,77]. Verapamil and lidocaine were able to reduce APD in another LQT model harbouring to variants (*KCNQ1* p.(Gly219Glu)/*TRPM4* p.(Thr160Met)) [78].

Table 3. Overview of published drug testing in iPSC-CM arrhythmia models.

Drug	Mode of Action	Disease Gene Mutation	Effect on Phenotype	Ref.
Mexiletine analogues	Class 1B antiarrhythmic drug, inhibits I_{Na}	LQT <i>SCN5A</i> p.(Phe1473Cys), p.(Asn406Lys)	Mexiletine: I_{NaL} inhibition and APD shortening at lower dose but modest prolongation at higher dose and proarrhythmic response Analogues 'MexA2' and 'MexA5': more potent and selective for I_{NaL} over I_{NaP} and I_{Kr} , Shortening of APD and suppression of arrhythmia Analogues '13, 14, 25': shortening of APD and no EADs	[76,77]

Table 3. Cont.

Drug	Mode of Action	Disease Gene Mutation	Effect on Phenotype	Ref.
Verapamil, Lidocaine	Calcium channel blocker Sodium channel blocker	LQT KCNQ1 p.(Gly219Glu)/ TRPM4 p.(Thr160Met)	Reduction in APD	[78]
Telmisartan, GW0742	Agonists of the PPAR δ pathway, stabilise the active PKA-phosphorylated state of hERG	LQT KCNH2 p.(Ala561Thr)	Reduction in APD50, APD90 and triangularisation	[79]
NS1643	Change the voltage dependence of inactivation of hERG	LQT KCNH2 p.(Ala561Thr)	Reductions in APD50, APD90 and triangularisation	[79]
Lumacaftor	Trafficking chaperone during protein folding	LQT KCNH2 Trafficking p.(Ala561Val), (IVS9-28A/G), p.(Asn633Ser), p.(Arg685Pro), p.(Gly604Ser) Synthesis p.(Ser428X), p.(Arg366X)	<i>Trafficking variants</i> Increased membrane localisation, reduced cFPD and APD90, increase in I _{Kr} current densities, reduced calcium transient irregularities and frequency p.(Gly604Ser): increased membrane expression, no effect on APD90 <i>Other variants</i> Reduced calcium transient irregularities and frequency, no effect on cFPD	[80,81]
ICA-105574	Type II I _{Kr} activator (impairs transition to the inactivated state)	LQT KCNH2 p.(Thr983Ile), p.(Ala422Thr)	Increased I _{Kr} , shortening APD/cFPD in patient and control, shortened calcium transient, at higher concentrations (10–30 μ M): cessation of the spontaneous calcium transients	[11,82]
Ajmaline	Class IA anti-arrhythmic drug inhibits I _{Na} , I _{to} or I _{Kr}	BrS Unknown mutation	No difference between patient and control	[83]
		BrS SCN10A p.(Arg1268Gln)/ p.(Arg1250Gln)	Prolonged APD50 and APD90, reduced APA and V _{max}	[84]
		BrS SCN1B p.(Leu210Pro)/ p.(Pro213Thr)	Reduced APA and V _{max}	[85]
Cilostazol, Milrinone	Phosphodiesterase III inhibitors, increase I _{Ca} and suppress I _{to}	BrS SCN5A p.(Ser1812X)	Reduction in I _{to} , decreased arrhythmic beating, no EAD- or EAD-triggered activities	[17]
Bisoprolol	Beta blocker	BrS CACNB2 p.(Ser142Phe)	Reduced arrhythmic events and reduced variation in the beat-to-beat interval time at 30 nM	[15]
Quinidine	Class I antiarrhythmic agent, blocking I _{to}	BrS CACNB2 p.(Ser142Phe)	Reduced arrhythmic events	[15]
		BrS SCN5A p.(Val1405Met) SCN1B p.(Ala197Val)	Elimination of arrhythmic events (EAD, DAD), V _{max} , APA, and RMP reduced in control and patients' groups	[16]
		SQT KCNH2 p.(Thr618Ile)	Prolonged APD	[20]
		SQT KCNH2 p.(Asn588Lys)	Reduced V _{max} , prolonged APD, elimination of arrhythmic events	[18]

Table 3. Cont.

Drug	Mode of Action	Disease Gene Mutation	Effect on Phenotype	Ref.
Toxin BmKKx2	Selective I _{Kr} blocker	SQT KCNH2 p.(Thr618Ile)	Prolonged APD	[20]
Ivabradine, Ajmaline, Mexiletine	Inhibitor of the pacemaker funny current Class IA anti-arrhythmic drug, inhibits I _{Na} , I _{to} or I _{Kr} Class 1B antiarrhythmic drug	SQT KCNH2 p.(Asn588Lys)	Prolonged APD90, reduced number of arrhythmic events	[86]
MiCUpS (efsevin, kaempferol, ezetimibe, disulfiram)	Mitochondrial Ca ²⁺ uptake enhancers	CPVT RYR2 p.(Ser406Leu)	Reduced number of cells displaying Ca ²⁺ waves and reduced frequency of Ca ²⁺ waves	[87]
		CPVT unknown mutation	Reduced Ca ²⁺ waves	[88]
Autocamide-2-related inhibitory peptide (AIP)	Ca ²⁺ /calmodulin-dependent protein kinase II (CaMKII) inhibitory peptide	CPVT RYR2 p.(Ser404Arg)/ p.(Asn658Ser), p.(Gly3946Ser)/ p.(Gly1885Glu)	Reduced abnormal Ca ²⁺ transients, reduced frequency of Ca ²⁺ sparks, restored regular and spontaneous Ca ²⁺ transients	[89]
Tetracaine derivative EL20	Targeted inhibition of RyR2	CPVT RYR2 p.(Arg176Gln)	Reduced the Ca ²⁺ spark frequency, prevented pacing-evoked Ca ²⁺ oscillations	[24]
Nadolol, Flecainide	Non-selective beta blocker Class IC anti-arrhythmic agent inhibits I _{Na} and I _{Kr}	CPVT RYR2 p.(Phe13Leu), p.(Leu14Pro), p.(Arg15Pro), p.(Arg176Gln)	Reduced Ca ²⁺ transient amplitude, reduced spontaneous Ca ²⁺ release, reduced Ca ²⁺ sparking activity, decreased irregularities in beat period and spontaneous beat rate	[26]

Several LQT2 models, with pathogenic variants in the *KCNH2* (hERG channel) have also been used to test drugs. Telmisartan and GW0742 are agonists of the PPAR δ pathway, which helps hERG to stabilise the PKA-phosphorylated active state of the channel opening at more negative potentials. Duncan et al. tested these agonists in a patient iPSC-CM model harbouring a *KCNH2* p.(Ala561Thr) variant and found a 20% reduction in APD for both compounds, which is comparable to the observed effect of NS1643 (also 20% APD shortening), a known compound that reduces inactivation of the hERG channel [79]. Mehta et al. created iPSC-CMs of five patients with either disrupted *KCNH2* trafficking (p.(Ala561Val), (IVS9-28A/G)) or synthesis (p.(Ser428X), p.(Arg366X)) to test the use of lumacaftor as a treatment option as the drug acts as a chaperone during protein folding. As predicted, they found higher *KCNH2* expression and shortened field potentials after 7 days of treatment with lumacaftor in patients with trafficking defect mutations but not in patients with disrupted synthesis of the hERG channel [80]. Two of the patients received treatment with lumacaftor and Ivacaftor and indeed showed a shorter QTc, however this shortening was not as pronounced as in the in vitro model indicating that the translation from in vitro to in vivo is not straightforward [90]. Another study also tested lumacaftor on three LQT2 (*KCNH2*) patient iPSC-CM lines with different pathogenic variants and found rescued phenotypes in two (p.(Asn633Ser), p.(Arg685Pro)) of the three lines. For the third one (p.(Gly604Ser)), on the other hand, they saw a prolongation of the AP after administration of the compound, which could be explained by the dominant-negative effect that was observed next to the trafficking defect caused by the third variant [81]. Another compound (ICA-105574, a type II I_{Kr} activator) was used by two groups and tested both on VUS (p.(Thr983Ile)) and pathogenic (p.(Ala422Thr)) LQT2 iPSC-CM models. They both saw a shortening of the action potential, field potential or calcium transient but with the risk of overcorrection at higher concentrations which might induce arrhythmic events [11,82].

Ajmaline is a class IA anti-arrhythmic drug that can be used to diagnose BrS patients. Studies have already shown that ajmaline can inhibit various currents, including I_{Na} , I_{to} or I_{Kr} [83]. In the iPSC-CM of a BrS patient without a known genetic cause ajmaline had the same blocking effect on both the repolarisation and depolarisation caused by an inhibition of both I_{Na} and I_{Kr} as observed in the control iPSC-CMs. In an iPSC-CM model harbouring two *SCN10A* (p.(Arg1268Gln)/p.(Arg1250Gln) variants there was a more pronounced reduction in APA and V_{max} compared to control iPSC-CMs [84]. The same was observed in a *SCN1B* (p.(Leu210Pro)/p.(Pro213Thr)) iPSC-CM model [85]. Cilostazol and milrinone, two phosphodiesterase III inhibitors, increased I_{Ca} and suppressed I_{to} by increasing the heart rate [91]. These were tested on BrS iPSC-CM models from two patients carrying a *SCN5A* p.(Ser1812X) variant, which resulted in a reduction in I_{to} and arrhythmic beating [17]. Bisoprolol, a beta blocker, was recently tested in a *CACNB2* p.(Ser142Phe) iPSC-CM model and reduced variation in beat-to-beat interval time as well as arrhythmic events. Quinidine, a class I antiarrhythmic agent, on the other hand, only reduced arrhythmic events [15]. The same anti-arrhythmic effect of quinidine was observed in a *SCN5A* (p.(Val1405Met)) and *SCN1B* (p.(Ala197Val)) iPSC-CM model [16].

Guo et al. tested quinidine in an iPSC-CM model of a SQT (*KCNH2*, p.(Thr618Ile)) patient who was already receiving quinidine treatment. The cell model confirmed the beneficial effect of quinidine as APD was prolonged, comparable to the APD of the isogenic control. Next to quinidine, a short peptide derived from a scorpion, BmKKx2, prolonged the APD by targeting the *KCNH2* gene [20]. In another model (*KCNH2* p.(Asn588Lys)), quinidine reduced V_{max} , prolonged APD and abolished arrhythmic events while sotalol and metoprolol did not have an effect [18]. Ivabradine, ajmaline, and mexiletine prolonged APD and reduced arrhythmic events in the same iPSC-CM model [86].

One way to prevent arrhythmias in CPVT is to upregulate the calcium uptake by the mitochondria by, for example, mitochondrial Ca^{2+} uptake enhancers (MiCUp) such as efsevin and kaempferol [87]. These MiCUps were tested both in mice and *RYR2* (p.(Ser406Leu)) patient iPSC-CMs and were able to reduce episodes of stress-induced ventricular tachycardia in mice and reduce arrhythmogenic Ca^{2+} waves in iPSC-CMs [87]. Two other MiCUps, ezetimibe and disulfiram, suppressed arrhythmogenesis in patient iPSC-CMs [88] (genetic variant not specified). Another way to modulate calcium is by inhibiting the Ca^{2+} /calmodulin-dependent protein kinase II (CaMKII) with a CaMKII inhibitory peptide, which is successful in reducing the abnormal Ca^{2+} release events and frequency of Ca^{2+} sparks in two CPVT *RYR2* (p.(Ser404Arg)/p.(Asn658Ser), p.(Gly3946Ser)/p.(Gly1885Glu)) iPSC-CMs [89]. EL20, a tetracaine derivative and *RYR2* inhibitor, decreased spark activity in iPSC-CMs of a CPVT patient harbouring a *RYR2* (p.(Arg176Gln)) mutation without negatively affecting the Ca^{2+} transient amplitude [24]. Stutzman et al. created four iPSC-CM lines of CPVT patients with *RYR2* mutations, (p.(Phe13Leu), p.(Leu14Pro), p.(Arg15Pro) and p.(Arg176Gln)), and treated them with nadolol and flecainide. Both were able to decrease the Ca^{2+} transient amplitude and spark activity [26].

All these reports confirm the great potential of iPSC-CM arrhythmia models to test novel and existing therapies, and also for personalised medicine. In both 2D and 3D, they could also be effectively used for larger drug-library screening experiments.

4.3. Gene Therapy Testing

Inherited cardiac arrhythmia iPSC-CM models have also been used to test novel gene therapies, acting straight on the nucleic acid molecular/genetic level.

One way to perform gene therapy is by patient-specific targeting the causal mutation. Matsa et al. used an allele-specific small interfering RNA to knock down the mutated *KCNH2* mRNA in LQTS (*KCNH2* p.(Ala561Thr)) patient iPSC-CMs thereby preventing the dominant negative-trafficking defect. This resulted in a shortening of the AP, increase in K^+ current and rescue of the arrhythmogenic phenotype [92]. A more general gene therapy approach was published by Dotzler et al. They developed a novel method with a dual mode of action called suppression-and-replacement (SupRep) *KCNQ1* gene therapy. As the name

indicates, first the endogenous alleles were suppressed by short hairpin RNA (shRNA) and in the next step, the *KCNQ1* gene was replaced by expression of a shRNA-immune (shIMM) *KCNQ1* cDNA immune for breakdown by the shRNA. This method was tested in four LQT1 (*KCNQ1* p.(Tyr171X), p.(Val254Met), p.(Ile567Ser) and p.(Ala344Ala/splice variant)) patient iPSC-CM models and showed a shortening of the APD in all 2D patient models. As a proof-of-concept, a 3D cardiac organoid of one of the patient lines (p.(Tyr171X)) was created and here as well, an APD shortening was observed after treatment [93]. The same treatment approach was used for *KCNH2* variants, in iPSC-CM models of two LQT2 (p.(Gly604Ser), p.(Asn633Ser)) patients as well as in one SQT (p.(Asn588Lys) patient and resulted in a normal APD90 for both the LQT2 and SQT patients [94].

5. Discussion and Conclusions

With the advent of iPSC creation, major steps have been taken to differentiate these stem cells into several cell types including iPSC-derived cardiomyocytes. Using this model in inherited cardiac arrhythmia research has increased knowledge on the underlying disease mechanisms and creates opportunities to functionally characterise and interpret the pathogenicity of patient-specific genetic variants and to perform (personalised) drug testing. As a proof-of-concept of this more 'personalised' drug testing, a few 'clinical trials in a dish' have been performed where healthy control individuals and their iPSC-CMs were challenged with known QT-prolonging drugs to compare the effect on the in vitro model to the in vivo situation. Using sotalol, a correlation was found between the in vivo QT interval and in vitro FPD results [95]. One study also found such a positive correlation for moxifloxacin [96] while another did not find a correlation between the APD response slopes and clinical QT response to moxifloxacin or dofetilide [97]. Using (subject-specific) iPSCs for research and drug testing also requires the use of a comprehensive informed consent explaining future use of created iPSCs and derivatives. The reported 2D iPSC-CM disease models recapitulate the patients' phenotype at the cellular level, however, if the specific tested characteristics are compared over several iPSC-clones or several different papers, quite some variability can be observed [98]. In addition, for example, the iPSC-CM models of BrS patients with an unknown genetic cause did not show any electrophysiological differences compared to healthy control iPSC-CMs [99]. The known immature phenotype of iPSC-CMs with immature ion channel expression most likely plays a role in these observations and small changes in ionic currents might not be picked up. More in-depth analysis of the iPSC-CM cellular disease phenotype including transcriptomics or proteomics approaches could be useful to further characterise these models.

In addition, efforts have been made to improve the maturity of iPSC-CMs, with one important strategy to culture them in 3D models such as microtissues, organoids and engineered heart tissue. Amongst others, Kerr et al. showed that iPSC-CM in 3D cultures showed a higher similarity to human adult myocardial transcriptome compared to 2D models and had enhanced cell–cell communication, ECM organisation and vascularisation capacity [100]. The addition of other (iPSC-derived) cell types that are present in heart tissue further improves the physiological relevance and maturation state of the model. Use of these 3D models will certainly increase the suitability for disease modelling and drug testing. It should be taken into account, though, that they are more complex at the culture level—complicating the high-throughput needed for larger screenings, so that extra variability is introduced to an already variable model [98] and the complexity of the analysis is also increased. Light for microscopy, fluorescent dyes and drugs need to penetrate deeper and evenly into the 3D culture to reach all cells, more computational power might be needed and more expensive single-cell analysis approaches such as scRNA-seq could be necessary. Indeed, Feng et al. already performed single cell analysis on cardiac organoids and found more differentially expressed genes in iPSC-CMs compared to other cell types present in the organoid between Ebstein's anomaly patients and healthy controls [101].

Despite the immense progress that has been made in iPSC-CM generation and application potential, some limiting factors such as immaturity, genetic and phenotypic

heterogeneity and variability still have an impact on their usability and should be kept in mind when translating the results in vivo [98]. For clinical application in regenerative medicine the arrhythmogenic potential, immunogenicity, tumorigenicity and heterogeneity of the iPSC-CMs should be taken into consideration. In conclusion, iPSC-CMs have been instrumental in modelling inherited cardiac arrhythmias, small-scale testing of disease-specific drugs or gene therapies and cardiotoxicity testing. The transition from 2D to 3D models has improved cellular maturity and physiological relevance, but also increases the complexity of the model and its analysis. Large-scale drug library screenings have not yet been performed, but further automation and high-throughput analysis methods will certainly pave the way for this application. Further evolution of both 2D and 3D iPSC-CM modelling and analysis techniques will allow the discovery of new treatment options for cardiac arrhythmias in general as well as for personalised medicine.

Supplementary Materials: The following are available online at <https://www.mdpi.com/article/10.3390/biomedicines11020334/s1>, Table S1: overview of previously published 2D iPSC-CM cardiac arrhythmia disease models. References [102–128] are cited.

Author Contributions: Conceptualization, E.S., M.A. and B.L.; Writing—original draft, E.S.; writing—review and editing, E.S., M.A. and B.L. All authors have read and agreed to the published version of the manuscript.

Funding: E. Simons is a research fellow supported by the Research Foundation—Flanders (FWO, Belgium, 1S25318N). Dr. Loeys holds a consolidator grant from the European Research Council (“Genomia” ERC-COG-2017-771945). This research was largely supported by funding from the University of Antwerp (GOA 33933; Methusalem-OEC grant “Genomed” 40709) and the Research Foundation Flanders (FWO, Belgium, G042321N, G040221N, G044720N).

Conflicts of Interest: The authors declare no conflict of interest.

References

1. Takahashi, K.; Yamanaka, S. Induction of Pluripotent Stem Cells from Mouse Embryonic and Adult Fibroblast Cultures by Defined Factors. *Cell* **2006**, *126*, 663–676. [CrossRef] [PubMed]
2. Iannielli, A.; Luoni, M.; Giannelli, S.G.; Ferese, R.; Ordazzo, G.; Fossati, M.; Raimondi, A.; Opazo, F.; Corti, O.; Prehn, J.H.M.; et al. Modeling native and seeded Synuclein aggregation and related cellular dysfunctions in dopaminergic neurons derived by a new set of isogenic iPSC lines with SNCA multiplications. *Cell Death Dis.* **2022**, *13*, 881. [CrossRef] [PubMed]
3. Zwi, L.; Caspi, O.; Arbel, G.; Huber, I.; Gepstein, A.; Park, I.-H.; Gepstein, L. Cardiomyocyte Differentiation of Human Induced Pluripotent Stem Cells. *Circulation* **2009**, *120*, 1513–1523. [CrossRef] [PubMed]
4. Lai, X.; Li, C.; Xiang, C.; Pan, Z.; Zhang, K.; Wang, L.; Xie, B.; Cao, J.; Shi, J.; Deng, J.; et al. Generation of functionally competent hepatic stellate cells from human stem cells to model liver fibrosis in vitro. *Stem Cell Rep.* **2022**, *17*, 2531–2547. [CrossRef]
5. Casini, S.; Verkerk, A.O.; Remme, C.A. Human iPSC-Derived Cardiomyocytes for Investigation of Disease Mechanisms and Therapeutic Strategies in Inherited Arrhythmia Syndromes: Strengths and Limitations. *Cardiovasc. Drugs Ther.* **2017**, *31*, 325–344. [CrossRef] [PubMed]
6. Moretti, A.; Bellin, M.; Welling, A.; Jung, C.B.; Lam, J.T.; Bott-Flügel, L.; Dorn, T.; Goedel, A.; Höhnke, C.; Hofmann, F.; et al. Patient-Specific Induced Pluripotent Stem-Cell Models for Long-QT Syndrome. *N. Engl. J. Med.* **2010**, *363*, 1397–1409. [CrossRef]
7. Rajamohan, D.; Kalra, S.; Hoang, M.D.; George, V.; Staniforth, A.; Russell, H.; Yang, X.; Denning, C. Automated Electrophysiological and Pharmacological Evaluation of Human Pluripotent Stem Cell-Derived Cardiomyocytes. *Stem Cells Dev.* **2016**, *25*, 439–452. [CrossRef]
8. Protze, S.L.; Lee, J.H.; Keller, G.M. Human Pluripotent Stem Cell-Derived Cardiovascular Cells: From Developmental Biology to Therapeutic Applications. *Cell Stem Cell* **2019**, *25*, 311–327. [CrossRef]
9. Garg, P.; Garg, V.; Shrestha, R.; Sanguinetti, M.C.; Kamp, T.J.; Wu, J.C. Human Induced Pluripotent Stem Cell-Derived Cardiomyocytes as Models for Cardiac Channelopathies. *Circ. Res.* **2018**, *123*, 224–243. [CrossRef]
10. Pan, Z.; Ebert, A.; Liang, P. Human-induced pluripotent stem cells as models for rare cardiovascular diseases: From evidence-based medicine to precision medicine. *Pflugers Arch.* **2021**, *473*, 1151–1165. [CrossRef]
11. Garg, P.; Oikonomopoulos, A.; Chen, H.; Li, Y.; Lam, C.K.; Sallam, K.; Perez, M.; Lux, R.L.; Sanguinetti, M.C.; Wu, J.C. Genome Editing of Induced Pluripotent Stem Cells to Decipher Cardiac Channelopathy Variant. *J. Am. Coll. Cardiol.* **2018**, *72*, 62–75. [CrossRef] [PubMed]
12. Chavali, N.V.; Kryshtal, D.O.; Parikh, S.S.; Wang, L.; Glazer, A.M.; Blackwell, D.J.; Kroncke, B.M.; Shoemaker, M.B.; Knollmann, B.C. Patient-independent human induced pluripotent stem cell model: A new tool for rapid determination of genetic variant pathogenicity in long QT syndrome. *Heart Rhythm.* **2019**, *16*, 1686–1695. [CrossRef] [PubMed]

13. Davis, R.P.; Casini, S.; Berg, C.W.V.D.; Hoekstra, M.; Remme, C.A.; Dambrot, C.; Salvatori, D.; Oostwaard, D.W.-V.; Wilde, A.A.M.; Bezzina, C.R.; et al. Cardiomyocytes Derived From Pluripotent Stem Cells Recapitulate Electrophysiological Characteristics of an Overlap Syndrome of Cardiac Sodium Channel Disease. *Circulation* **2012**, *125*, 3079–3091. [[CrossRef](#)] [[PubMed](#)]
14. Liang, P.; Sallam, K.; Wu, H.; Li, Y.; Itzhaki, I.; Garg, P.; Zhang, Y.; Termglichen, V.; Lan, F.; Gu, M.; et al. Patient-Specific and Genome-Edited Induced Pluripotent Stem Cell-Derived Cardiomyocytes Elucidate Single-Cell Phenotype of Brugada Syndrome. *J. Am. Coll. Cardiol.* **2016**, *68*, 2086–2096. [[CrossRef](#)] [[PubMed](#)]
15. Zhong, R.; Schimanski, T.; Zhang, F.; Lan, H.; Hohn, A.; Xu, Q.; Huang, M.; Liao, Z.; Qiao, L.; Yang, Z.; et al. A Preclinical Study on Brugada Syndrome with a CACNB2 Variant Using Human Cardiomyocytes from Induced Pluripotent Stem Cells. *Int. J. Mol. Sci.* **2022**, *23*, 8313. [[CrossRef](#)]
16. Zhu, Y.; Wang, L.; Cui, C.; Qin, H.; Chen, H.; Chen, S.; Lin, Y.; Cheng, H.; Jiang, X.; Chen, M. Pathogenesis and drug response of iPSC-derived cardiomyocytes from two Brugada syndrome patients with different Nav1.5-subunit mutations. *J. Biomed. Res.* **2021**, *35*, 395. [[CrossRef](#)]
17. Li, W.; Stauske, M.; Luo, X.; Wagner, S.; Vollrath, M.; Mehnert, C.S.; Schubert, M.; Cyganek, L.; Chen, S.; Hasheminasab, S.-M.; et al. Disease Phenotypes and Mechanisms of iPSC-Derived Cardiomyocytes From Brugada Syndrome Patients With a Loss-of-Function SCN5A Mutation. *Front. Cell Dev. Biol.* **2020**, *8*, 592893. [[CrossRef](#)]
18. El-Battrawy, I.; Lan, H.; Cyganek, L.; Zhao, Z.; Li, X.; Buljubasic, F.; Lang, S.; Yücel, G.; Sattler, K.; Zimmermann, W.; et al. Modeling Short QT Syndrome Using Human-Induced Pluripotent Stem Cell-Derived Cardiomyocytes. *J. Am. Heart Assoc.* **2018**, *7*, e007394. [[CrossRef](#)]
19. Shinnawi, R.; Shaheen, N.; Huber, I.; Shiti, A.; Arbel, G.; Gepstein, A.; Ballan, N.; Setter, N.; Tijssen, A.J.; Borggreffe, M.; et al. Modeling Reentry in the Short QT Syndrome With Human-Induced Pluripotent Stem Cell-Derived Cardiac Cell Sheets. *J. Am. Coll. Cardiol.* **2019**, *73*, 2310–2324. [[CrossRef](#)]
20. Guo, F.; Sun, Y.; Wang, X.; Wang, H.; Wang, J.; Gong, T.; Chen, X.; Zhang, P.; Su, L.; Fu, G.; et al. Patient-Specific and Gene-Corrected Induced Pluripotent Stem Cell-Derived Cardiomyocytes Elucidate Single-Cell Phenotype of Short QT Syndrome. *Circ. Res.* **2019**, *124*, 66–78. [[CrossRef](#)]
21. Fatima, A.; Xu, G.; Shao, K.; Papadopoulos, S.; Lehmann, M.; Arnáiz-Cot, J.J.; Rosa, A.O.; Nguemo, F.; Matzkies, M.; Dittmann, S.; et al. In vitro Modeling of Ryanodine Receptor 2 Dysfunction Using Human Induced Pluripotent Stem Cells. *Cell. Physiol. Biochem.* **2011**, *28*, 579–592. [[CrossRef](#)] [[PubMed](#)]
22. Wei, H.; Zhang, X.-H.; Clift, C.; Yamaguchi, N.; Morad, M. CRISPR/Cas9 Gene editing of RyR2 in human stem cell-derived cardiomyocytes provides a novel approach in investigating dysfunctional Ca²⁺ signaling. *Cell Calcium* **2018**, *73*, 104–111. [[CrossRef](#)] [[PubMed](#)]
23. Acimovic, I.; Refaat, M.M.; Moreau, A.; Salykin, A.; Reiken, S.; Sleiman, Y.; Souidi, M.; Příbyl, J.; Kajava, A.V.; Richard, S.; et al. Post-Translational Modifications and Diastolic Calcium Leak Associated to the Novel RyR2-D3638A Mutation Lead to CPVT in Patient-Specific hiPSC-Derived Cardiomyocytes. *J. Clin. Med.* **2018**, *7*, 423. [[CrossRef](#)] [[PubMed](#)]
24. Word, T.A.; Quick, A.P.; Miyake, C.Y.; Shak, M.K.; Pan, X.; Kim, J.J.; Allen, H.D.; Sibrian-Vazquez, M.; Strongin, R.M.; Landstrom, A.P.; et al. Efficacy of RyR2 inhibitor EL20 in induced pluripotent stem cell-derived cardiomyocytes from a patient with catecholaminergic polymorphic ventricular tachycardia. *J. Cell. Mol. Med.* **2021**, *25*, 6115–6124. [[CrossRef](#)]
25. Zhang, X.-H.; Wei, H.; Xia, Y.; Morad, M. Calcium signaling consequences of RyR2 mutations associated with CPVT1 introduced via CRISPR/Cas9 gene editing in human-induced pluripotent stem cell-derived cardiomyocytes: Comparison of RyR2-R420Q, F2483I, and Q4201R. *Heart Rhythm.* **2021**, *18*, 250–260. [[CrossRef](#)]
26. Stutzman, M.J.; Kim, C.J.; Tester, D.J.; Hamrick, S.K.; Dotzler, S.M.; Giudicessi, J.R.; Miotto, M.C.; Gc, J.B.; Frank, J.; Marks, A.R.; et al. Characterization of N-terminal RYR2 variants outside CPVT1 hotspot regions using patient iPSCs reveal pathogenesis and therapeutic potential. *Stem Cell Rep.* **2022**, *17*, 2023–2036. [[CrossRef](#)]
27. Novak, A.; Barad, L.; Zeevi-Levin, N.; Shick, R.; Shtrichman, R.; Lorber, A.; Itskovitz-Eldor, J.; Binah, O. Cardiomyocytes generated from CPVT-D307H patients are arrhythmogenic in response to β -adrenergic stimulation. *J. Cell. Mol. Med.* **2012**, *16*, 468–482. [[CrossRef](#)]
28. Ma, D.; Wei, H.; Lu, J.; Ho, S.; Zhang, G.; Sun, X.; Oh, Y.; Tan, S.H.; Ng, M.L.; Shim, W.; et al. Generation of patient-specific induced pluripotent stem cell-derived cardiomyocytes as a cellular model of arrhythmogenic right ventricular cardiomyopathy. *Eur. Heart J.* **2013**, *34*, 1122–1133. [[CrossRef](#)]
29. El-Battrawy, I.; Zhao, Z.; Lan, H.; Cyganek, L.; Tombers, C.; Li, X.; Buljubasic, F.; Lang, S.; Tiburcy, M.; Zimmermann, W.-H.; et al. Electrical dysfunctions in human-induced pluripotent stem cell-derived cardiomyocytes from a patient with an arrhythmogenic right ventricular cardiomyopathy. *Europace* **2018**, *20*, f46–f56. [[CrossRef](#)]
30. Buljubasic, F.; El-Battrawy, I.; Lan, H.; Lomada, S.K.; Chatterjee, A.; Zhao, Z.; Li, X.; Zhong, R.; Xu, Q.; Huang, M.; et al. Nucleoside Diphosphate Kinase B Contributes to Arrhythmogenesis in Human-Induced Pluripotent Stem Cell-Derived Cardiomyocytes from a Patient with Arrhythmogenic Right Ventricular Cardiomyopathy. *J. Clin. Med.* **2020**, *9*, 486. [[CrossRef](#)]
31. Priori, S.G.; Blomström-Lundqvist, C.; Mazzanti, A.; Blom, N.; Borggreffe, M.; Camm, J.; Elliott, P.M.; Fitzsimons, D.; Hatala, R.; Hindricks, G.; et al. 2015 ESC Guidelines for the management of patients with ventricular arrhythmias and the prevention of sudden cardiac death: The Task Force for the Management of Patients with Ventricular Arrhythmias and the Prevention of Sudden Cardiac Death of the European Society of Cardiology (ESC). Endorsed by: Association for European Paediatric and Congenital Cardiology (AEPC). *Eur. Heart J.* **2015**, *36*, 2793–2867. [[CrossRef](#)]

32. Ponce-Balbuena, D.; Deschênes, I. Long QT syndrome—Bench to bedside. *Heart Rhythm. O2* **2021**, *2*, 89–106. [[CrossRef](#)]
33. Cerrone, M.; Costa, S.; Delmar, M. The Genetics of Brugada Syndrome. *Annu. Rev. Genom. Hum. Genet.* **2022**, *23*, 255–274. [[CrossRef](#)]
34. Vutthikraivit, W.; Rattanawong, P.; Putthapiban, P.; Sukhumthamarat, W.; Vathesatogkit, P.; Ngarmukos, T.; Thakkinstian, A. Worldwide Prevalence of Brugada Syndrome: A Systematic Review and Meta-Analysis. *Acta Cardiol. Sin.* **2018**, *34*, 267–277. [[CrossRef](#)]
35. Nijak, A.; Saenen, J.; Labro, A.; Schepers, D.; Loeys, B.; Alaerts, M. iPSC-Cardiomyocyte Models of Brugada Syndrome—Achievements, Challenges and Future Perspectives. *Int. J. Mol. Sci.* **2021**, *22*, 2825. [[CrossRef](#)]
36. Campuzano, O.; Sarquella-Brugada, G.; Cesar, S.; Arbelo, E.; Brugada, J.; Brugada, R. Recent Advances in Short QT Syndrome. *Front. Cardiovasc. Med.* **2018**, *5*, 149. [[CrossRef](#)] [[PubMed](#)]
37. Walsh, R.; Adler, A.; Amin, A.S.; Abiusi, E.; Care, M.; Bikker, H.; Amenta, S.; Feilotter, H.; Nannenber, E.A.; Mazzarotto, F.; et al. Evaluation of gene validity for CPVT and short QT syndrome in sudden arrhythmic death. *Eur. Heart J.* **2022**, *43*, 1500–1510. [[CrossRef](#)]
38. Leenhardt, A.; Denjoy, I.; Guicheney, P. Catecholaminergic Polymorphic Ventricular Tachycardia. *Circ. Arrhythmia Electrophysiol.* **2012**, *5*, 1044–1052. [[CrossRef](#)]
39. Corrado, D.; Basso, C.; Judge, D.P. Arrhythmogenic Cardiomyopathy. *Circ. Res.* **2017**, *121*, 784–802. [[CrossRef](#)]
40. Ahmed, R.E.; Anzai, T.; Chanthra, N.; Uosaki, H. A Brief Review of Current Maturation Methods for Human Induced Pluripotent Stem Cells-Derived Cardiomyocytes. *Front. Cell Dev. Biol.* **2020**, *8*, 178. [[CrossRef](#)]
41. Litviňuková, M.; Talavera-López, C.; Maatz, H.; Reichart, D.; Worth, C.L.; Lindberg, E.L.; Kanda, M.; Polanski, K.; Heinig, M.; Lee, M.; et al. Cells of the adult human heart. *Nature* **2020**, *588*, 466–472. [[CrossRef](#)]
42. Pinto, A.R.; Ilinykh, A.; Ivey, M.J.; Kuwabara, J.T.; D’Antoni, M.L.; Debuque, R.; Chandran, A.; Wang, L.; Arora, K.; Rosenthal, N.; et al. Revisiting Cardiac Cellular Composition. *Circ. Res.* **2016**, *118*, 400–409. [[CrossRef](#)] [[PubMed](#)]
43. Bai, Y.; Yeung, E.; Lui, C.; Ong, C.S.; Pitaktong, I.; Huang, C.; Inoue, T.; Matsushita, H.; Ma, C.; Hibino, N. A Net Mold-based Method of Scaffold-free Three-Dimensional Cardiac Tissue Creation. *J. Vis. Exp.* **2018**, e58252. [[CrossRef](#)]
44. Sharma, P.; Gentile, C. Cardiac Spheroids as in vitro Bioengineered Heart Tissues to Study Human Heart Pathophysiology. *J. Vis. Exp.* **2021**, e61962. [[CrossRef](#)]
45. Beauchamp, P.; Moritz, W.; Kelm, J.M.; Ullrich, N.; Agarkova, I.; Anson, B.D.; Suter, T.M.; Zuppinger, C. Development and Characterization of a Scaffold-Free 3D Spheroid Model of Induced Pluripotent Stem Cell-Derived Human Cardiomyocytes. *Tissue Eng. Part C Methods* **2015**, *21*, 852–861. [[CrossRef](#)] [[PubMed](#)]
46. Ergir, E.; La Cruz, J.O.-D.; Fernandes, S.; Cassani, M.; Niro, F.; Pereira-Sousa, D.; Vrbský, J.; Vinarský, V.; Perestrelo, A.R.; Debellis, D.; et al. Generation and maturation of human iPSC-derived 3D organotypic cardiac microtissues in long-term culture. *Sci. Rep.* **2022**, *12*, 17409. [[CrossRef](#)]
47. Drakhlis, L.; Biswanath, S.; Farr, C.-M.; Lupanow, V.; Teske, J.; Ritzenhoff, K.; Franke, A.; Manstein, F.; Bolesani, E.; Kempf, H.; et al. Human heart-forming organoids recapitulate early heart and foregut development. *Nat. Biotechnol.* **2021**, *39*, 737–746. [[CrossRef](#)] [[PubMed](#)]
48. Lewis-Israeli, Y.R.; Wasserman, A.H.; Gabalski, M.A.; Volmert, B.D.; Ming, Y.; Ball, K.A.; Yang, W.; Zou, J.; Ni, G.; Pajares, N.; et al. Self-assembling human heart organoids for the modeling of cardiac development and congenital heart disease. *Nat. Commun.* **2021**, *12*, 5142. [[CrossRef](#)]
49. Lee, S.-G.; Kim, Y.-J.; Son, M.-Y.; Oh, M.-S.; Kim, J.; Ryu, B.; Kang, K.-R.; Baek, J.; Chung, G.; Woo, D.H.; et al. Generation of human iPSCs derived heart organoids structurally and functionally similar to heart. *Biomaterials* **2022**, *290*, 121860. [[CrossRef](#)]
50. Giacomelli, E.; Meraviglia, V.; Campostrini, G.; Cochrane, A.; Cao, X.; van Helden, R.W.; Garcia, A.K.; Mircea, M.; Kostidis, S.; Davis, R.P.; et al. Human-iPSC-Derived Cardiac Stromal Cells Enhance Maturation in 3D Cardiac Microtissues and Reveal Non-cardiomyocyte Contributions to Heart Disease. *Cell Stem Cell* **2020**, *26*, 862–879. [[CrossRef](#)]
51. Prajapati, C.; Ojala, M.; Lappi, H.; Aalto-Setälä, K.; Pekkanen-Mattila, M. Electrophysiological evaluation of human induced pluripotent stem cell-derived cardiomyocytes obtained by different methods. *Stem Cell Res.* **2021**, *51*, 102176. [[CrossRef](#)]
52. Giacomelli, E.; Sala, L.; Oostwaard, D.W.-V.; Bellin, M. Cardiac microtissues from human pluripotent stem cells recapitulate the phenotype of long-QT syndrome. *Biochem. Biophys. Res. Commun.* **2021**, *572*, 118–124. [[CrossRef](#)]
53. Goldfracht, I.; Efraim, Y.; Shinnawi, R.; Kovalev, E.; Huber, I.; Gepstein, A.; Arbel, G.; Shaheen, N.; Tiburcy, M.; Zimmermann, W.H.; et al. Engineered heart tissue models from hiPSC-derived cardiomyocytes and cardiac ECM for disease modeling and drug testing applications. *Acta Biomater.* **2019**, *92*, 145–159. [[CrossRef](#)]
54. Fong, A.H.; Romero-López, M.; Heylman, C.M.; Keating, M.; Tran, D.; Sobrino, A.; Tran, A.Q.; Pham, H.H.; Fimbres, C.; Gershon, P.D.; et al. Three-Dimensional Adult Cardiac Extracellular Matrix Promotes Maturation of Human Induced Pluripotent Stem Cell-Derived Cardiomyocytes. *Tissue Eng. Part A* **2016**, *22*, 1016–1025. [[CrossRef](#)]
55. Zhang, M.; Xu, Y.; Chen, Y.; Yan, Q.; Li, X.; Ding, L.; Wei, T.; Zeng, D. Three-Dimensional Poly-(ϵ -Caprolactone) Nanofibrous Scaffolds Promote the Maturation of Human Pluripotent Stem Cells-Induced Cardiomyocytes. *Front. Cell Dev. Biol.* **2022**, *10*, 875278. [[CrossRef](#)]
56. Chen, Y.; Chan, J.P.Y.; Wu, J.; Li, R.; Santerre, J.P. Compatibility and function of human induced pluripotent stem cell derived cardiomyocytes on an electrospun nanofibrous scaffold, generated from an ionomeric polyurethane composite. *J. Biomed. Mater. Res. Part A* **2022**, *110*, 1932–1943. [[CrossRef](#)]

57. Sacchetto, C.; Vitiello, L.; De Windt, L.J.; Rampazzo, A.; Calore, M. Modeling Cardiovascular Diseases with hiPSC-Derived Cardiomyocytes in 2D and 3D Cultures. *Int. J. Mol. Sci.* **2020**, *21*, 3404. [[CrossRef](#)]
58. Lemoine, M.D.; Mannhardt, I.; Breckwoldt, K.; Prondzynski, M.; Flenner, F.; Ulmer, B.; Hirt, M.N.; Neuber, C.; Horváth, A.; Kloth, B.; et al. Human iPSC-derived cardiomyocytes cultured in 3D engineered heart tissue show physiological upstroke velocity and sodium current density. *Sci. Rep.* **2017**, *7*, 5464. [[CrossRef](#)]
59. Ronaldson-Bouchard, K.; Ma, S.P.; Yeager, K.; Chen, T.; Song, L.; Sirabella, D.; Morikawa, K.; Teles, D.; Yazawa, M.; Vunjak-Novakovic, G. Advanced maturation of human cardiac tissue grown from pluripotent stem cells. *Nature* **2018**, *556*, 239–243. [[CrossRef](#)]
60. Lu, K.; Seidel, T.; Cao-Ehlker, X.; Dorn, T.; Batcha, A.M.N.; Schneider, C.M.; Semmler, M.; Volk, T.; Moretti, A.; Dendorfer, A.; et al. Progressive stretch enhances growth and maturation of 3D stem-cell-derived myocardium. *Theranostics* **2021**, *11*, 6138–6153. [[CrossRef](#)]
61. Yang, Q.; Xiao, Z.; Lv, X.; Zhang, T.; Liu, H. Fabrication and Biomedical Applications of Heart-on-a-chip. *Int. J. Bioprint* **2021**, *7*, 370. [[CrossRef](#)]
62. Varzideh, F.; Mone, P.; Santulli, G. Bioengineering Strategies to Create 3D Cardiac Constructs from Human Induced Pluripotent Stem Cells. *Bioengineering* **2022**, *9*, 168. [[CrossRef](#)]
63. Paloschi, V.; Sabater-Lleal, M.; Middelkamp, H.; Vivas, A.; Johansson, S.; van der Meer, A.; Tenje, M.; Maegdefessel, L. Organ-on-a-chip technology: A novel approach to investigate cardiovascular diseases. *Cardiovasc. Res.* **2021**, *117*, 2742–2754. [[CrossRef](#)]
64. Liu, H.; Bolonduro, O.A.; Hu, N.; Ju, J.; Rao, A.A.; Duffy, B.M.; Huang, Z.; Black, L.D.; Timko, B.P. Heart-on-a-Chip Model with Integrated Extra- and Intracellular Bioelectronics for Monitoring Cardiac Electrophysiology under Acute Hypoxia. *Nano Lett.* **2020**, *20*, 2585–2593. [[CrossRef](#)]
65. Conant, G.; Lai, B.F.L.; Lu, R.X.Z.; Korolj, A.; Wang, E.Y.; Radisic, M. High-Content Assessment of Cardiac Function Using Heart-on-a-Chip Devices as Drug Screening Model. *Stem Cell Rev. Rep.* **2017**, *13*, 335–346. [[CrossRef](#)]
66. Zhao, Y.; Rafatian, N.; Wang, E.Y.; Wu, Q.; Lai, B.F.; Lu, R.X.; Savoji, H.; Radisic, M. Towards chamber specific heart-on-a-chip for drug testing applications. *Adv. Drug Deliv. Rev.* **2020**, *165–166*, 60–76. [[CrossRef](#)]
67. Colatsky, T.; Fermini, B.; Gintant, G.; Pierson, J.B.; Sager, P.; Sekino, Y.; Strauss, D.G.; Stockbridge, N. The Comprehensive in Vitro Proarrhythmia Assay (CiPA) initiative—Update on progress. *J. Pharmacol. Toxicol. Methods* **2016**, *81*, 15–20. [[CrossRef](#)]
68. Blinova, K.; Stohlman, J.; Vicente, J.; Chan, D.; Johannesen, L.; Hortigon-Vinagre, M.P.; Zamora, V.; Smith, G.; Crumb, W.J.; Pang, L.; et al. Comprehensive Translational Assessment of Human-Induced Pluripotent Stem Cell Derived Cardiomyocytes for Evaluating Drug-Induced Arrhythmias. *Toxicol. Sci.* **2017**, *155*, 234–247. [[CrossRef](#)]
69. Millard, D.; Dang, Q.; Shi, H.; Zhang, X.; Strock, C.; Kraushaar, U.; Zeng, H.; Levesque, P.; Lu, H.-R.; Guillon, J.-M.; et al. Cross-Site Reliability of Human Induced Pluripotent stem cell-derived Cardiomyocyte Based Safety Assays Using Microelectrode Arrays: Results from a Blinded CiPA Pilot Study. *Toxicol. Sci.* **2018**, *164*, 550–562. [[CrossRef](#)]
70. Kitaguchi, T.; Moriyama, Y.; Taniguchi, T.; Ojima, A.; Ando, H.; Uda, T.; Otabe, K.; Oguchi, M.; Shimizu, S.; Saito, H.; et al. CSAHi study: Evaluation of multi-electrode array in combination with human iPSC-derived cardiomyocytes to predict drug-induced QT prolongation and arrhythmia—Effects of 7 reference compounds at 10 facilities. *J. Pharmacol. Toxicol. Methods* **2016**, *78*, 93–102. [[CrossRef](#)]
71. Yamamoto, W.; Asakura, K.; Ando, H.; Taniguchi, T.; Ojima, A.; Uda, T.; Osada, T.; Hayashi, S.; Kasai, C.; Miyamoto, N.; et al. Electrophysiological Characteristics of Human iPSC-Derived Cardiomyocytes for the Assessment of Drug-Induced Proarrhythmic Potential. *PLoS ONE* **2016**, *11*, e0167348. [[CrossRef](#)]
72. Lee, S.-G.; Kim, J.; Oh, M.-S.; Ryu, B.; Kang, K.-R.; Baek, J.; Lee, J.-M.; Choi, S.-O.; Kim, C.-Y.; Chung, H.M. Development and validation of dual-cardiotoxicity evaluation method based on analysis of field potential and contractile force of human iPSC-derived cardiomyocytes / multielectrode assay platform. *Biochem. Biophys. Res. Commun.* **2021**, *555*, 67–73. [[CrossRef](#)]
73. Visone, R.; Lozano-Juan, F.; Marzorati, S.; Rivolta, M.W.; Pesenti, E.; Redaelli, A.; Sassi, R.; Rasponi, M.; Occhetta, P. Predicting human cardiac QT alterations and pro-arrhythmic effects of compounds with a 3D beating heart-on-chip platform. *Toxicol. Sci.* **2022**, *191*, 47–60. [[CrossRef](#)]
74. Charwat, V.; Charrez, B.; Siemons, B.A.; Finsberg, H.; Jæger, K.H.; Edwards, A.G.; Huebsch, N.; Wall, S.; Miller, E.; Tveito, A.; et al. Validating the Arrhythmogenic Potential of High-, Intermediate-, and Low-Risk Drugs in a Human-Induced Pluripotent Stem Cell-Derived Cardiac Microphysiological System. *ACS Pharmacol. Transl. Sci.* **2022**, *5*, 652–667. [[CrossRef](#)]
75. McKeithan, W.L.; Savchenko, A.; Yu, M.S.; Cerignoli, F.; Bruyneel, A.A.N.; Price, J.H.; Colas, A.R.; Miller, E.W.; Cashman, J.R.; Mercola, M. An Automated Platform for Assessment of Congenital and Drug-Induced Arrhythmia with hiPSC-Derived Cardiomyocytes. *Front. Physiol.* **2017**, *8*, 766. [[CrossRef](#)]
76. McKeithan, W.L.; Feyen, D.A.; Bruyneel, A.A.; Okolotowicz, K.J.; Ryan, D.A.; Sampson, K.J.; Potet, F.; Savchenko, A.; Gómez-Galeno, J.; Vu, M.; et al. Reengineering an Antiarrhythmic Drug Using Patient hiPSC Cardiomyocytes to Improve Therapeutic Potential and Reduce Toxicity. *Cell Stem Cell* **2020**, *27*, 813–821.e6. [[CrossRef](#)]
77. Johnson, M.; Gomez-Galeno, J.; Ryan, D.; Okolotowicz, K.; McKeithan, W.L.; Sampson, K.J.; Kass, R.S.; Mercola, M.; Cashman, J.R. Human iPSC-derived cardiomyocytes and pyridyl-phenyl mexiletine analogs. *Bioorg. Med. Chem. Lett.* **2021**, *46*, 128162. [[CrossRef](#)]
78. Wang, F.; Han, Y.; Sang, W.; Wang, L.; Liang, X.; Wang, L.; Xing, Q.; Guo, Y.; Zhang, J.; Zhang, L.; et al. In Vitro Drug Screening Using iPSC-Derived Cardiomyocytes of a Long QT-Syndrome Patient Carrying KCNQ1 & TRPM4 Dual Mutation: An Experimental Personalized Treatment. *Cells* **2022**, *11*, 2495. [[CrossRef](#)]

79. Duncan, G.; Firth, K.; George, V.; Hoang, M.D.; Staniforth, A.; Smith, G.; Denning, C. Drug-Mediated Shortening of Action Potentials in LQTS2 Human Induced Pluripotent Stem Cell-Derived Cardiomyocytes. *Stem Cells Dev.* **2017**, *26*, 1695–1705. [[CrossRef](#)]
80. Mehta, A.; Ramachandra, C.J.A.; Singh, P.; Chitre, A.; Lua, C.H.; Mura, M.; Crotti, L.; Wong, P.; Schwartz, P.J.; Gneccchi, M.; et al. Identification of a targeted and testable antiarrhythmic therapy for long-QT syndrome type 2 using a patient-specific cellular model. *Eur. Heart J.* **2018**, *39*, 1446–1455. [[CrossRef](#)]
81. O'Hare, B.J.; Kim, C.J.; Hamrick, S.K.; Ye, D.; Tester, D.J.; Ackerman, M.J. Promise and Potential Peril With Lumacaftor for the Trafficking Defective Type 2 Long-QT Syndrome-Causative Variants, p.G604S, p.N633S, and p.R685P, Using Patient-Specific Re-Engineered Cardiomyocytes. *Circ. Genom. Precis. Med.* **2020**, *13*, 466–475. [[CrossRef](#)]
82. Perry, M.D.; Ng, C.A.; Mangala, M.M.; Ng, T.Y.M.; Hines, A.D.; Liang, W.; Xu, M.J.O.; Hill, A.P.; Vandenberg, J.I. Pharmacological activation of IKr in models of long QT Type 2 risks overcorrection of repolarization. *Cardiovasc. Res.* **2019**, *116*, 1434–1445. [[CrossRef](#)]
83. Miller, D.C.; Harmer, S.C.; Poliandri, A.; Nobles, M.; Edwards, E.C.; Ware, J.S.; Sharp, T.V.; McKay, T.R.; Dunkel, L.; Lambiase, P.D.; et al. Ajmaline blocks I Na and I Kr without eliciting differences between Brugada syndrome patient and control human pluripotent stem cell-derived cardiac clusters. *Stem Cell Res.* **2017**, *25*, 233–244. [[CrossRef](#)]
84. El-Battrawy, I.; Albers, S.; Cyganek, L.; Zhao, Z.; Lan, H.; Li, X.; Xu, Q.; Kleinsorge, M.; Huang, M.; Liao, Z.; et al. A cellular model of Brugada syndrome with SCN10A variants using human-induced pluripotent stem cell-derived cardiomyocytes. *Europace* **2019**, *21*, 1410–1421. [[CrossRef](#)]
85. El-Battrawy, I.; Müller, J.; Zhao, Z.; Cyganek, L.; Zhong, R.; Zhang, F.; Kleinsorge, M.; Lan, H.; Li, X.; Xu, Q.; et al. Studying Brugada Syndrome With an SCN1B Variants in Human-Induced Pluripotent Stem Cell-Derived Cardiomyocytes. *Front. Cell Dev. Biol.* **2019**, *7*, 261. [[CrossRef](#)]
86. Zhao, Z.; Li, X.; El-Battrawy, I.; Lan, H.; Zhong, R.; Xu, Q.; Huang, M.; Liao, Z.; Lang, S.; Zimmermann, W.; et al. Drug Testing in Human-Induced Pluripotent Stem Cell-Derived Cardiomyocytes From a Patient With Short QT Syndrome Type 1. *Clin. Pharmacol. Ther.* **2019**, *106*, 642–651. [[CrossRef](#)]
87. Schweitzer, M.K.; Wilting, F.; Sedej, S.; Dreizehnter, L.; Dupper, N.J.; Tian, Q.; Moretti, A.; My, I.; Kwon, O.; Priori, S.G.; et al. Suppression of Arrhythmia by Enhancing Mitochondrial Ca²⁺ Uptake in Catecholaminergic Ventricular Tachycardia Models. *JACC Basic Transl. Sci.* **2017**, *2*, 737–747. [[CrossRef](#)]
88. Sander, P.; Feng, M.; Schweitzer, M.K.; Wilting, F.; Gutenthaler, S.M.; Arduino, D.M.; Fischbach, S.; Dreizehnter, L.; Moretti, A.; Gudermann, T.; et al. Approved drugs ezetimibe and disulfiram enhance mitochondrial Ca²⁺ uptake and suppress cardiac arrhythmogenesis. *Br. J. Pharmacol.* **2021**, *178*, 4518–4532. [[CrossRef](#)]
89. Bezzerides, V.J.; Caballero, A.; Wang, S.; Ai, Y.; Hyland, R.J.; Lu, F.; Heims-Waldron, D.A.; Chambers, K.D.; Zhang, D.; Abrams, D.J.; et al. Gene Therapy for Catecholaminergic Polymorphic Ventricular Tachycardia by Inhibition of Ca²⁺ /Calmodulin-Dependent Kinase II. *Circulation* **2019**, *140*, 405–419. [[CrossRef](#)]
90. Schwartz, P.J.; Gneccchi, M.; Dagradi, F.; Castelletti, S.; Parati, G.; Spazzolini, C.; Sala, L.; Crotti, L. From patient-specific induced pluripotent stem cells to clinical translation in long QT syndrome Type 2. *Eur. Heart J.* **2019**, *40*, 1832–1836. [[CrossRef](#)]
91. Li, Y.; Lang, S.; Akin, I.; Zhou, X.; El-Battrawy, I. Brugada Syndrome: Different Experimental Models and the Role of Human Cardiomyocytes From Induced Pluripotent Stem Cells. *J. Am. Heart Assoc.* **2022**, *11*, e024410. [[CrossRef](#)] [[PubMed](#)]
92. Matsa, E.; Dixon, J.E.; Medway, C.; Georgiou, O.; Patel, M.J.; Morgan, K.; Kemp, P.J.; Staniforth, A.; Mellor, I.; Denning, C. Allele-specific RNA interference rescues the long-QT syndrome phenotype in human-induced pluripotency stem cell cardiomyocytes. *Eur. Heart J.* **2014**, *35*, 1078–1087. [[CrossRef](#)]
93. Dotzler, S.M.; Kim, C.J.; Gendron, W.A.; Zhou, W.; Ye, D.; Bos, J.M.; Tester, D.J.; Barry, M.A.; Ackerman, M.J. Suppression-Replacement *KCNQ1* Gene Therapy for Type 1 Long QT Syndrome. *Circulation* **2021**, *143*, 1411–1425. [[CrossRef](#)] [[PubMed](#)]
94. Bains, S.; Zhou, W.; Dotzler, S.M.; Martinez, K.; Kim, C.J.; Tester, D.J.; Ye, D.; Ackerman, M.J. Suppression and Replacement Gene Therapy for *KCNH2* -Mediated Arrhythmias. *Circ. Genom. Precis. Med.* **2022**, *15*, e003719. [[CrossRef](#)] [[PubMed](#)]
95. Stillitano, F.; Hansen, J.; Kong, C.-W.; Karakikes, I.; Funck-Brentano, C.; Geng, L.; Scott, S.; Reynier, S.; Wu, M.; Valogne, Y.; et al. Modeling susceptibility to drug-induced long QT with a panel of subject-specific induced pluripotent stem cells. *eLife* **2017**, *6*, e19406. [[CrossRef](#)]
96. Shinozawa, T.; Nakamura, K.; Shoji, M.; Morita, M.; Kimura, M.; Furukawa, H.; Ueda, H.; Shiramoto, M.; Matsuguma, K.; Kaji, Y.; et al. Recapitulation of Clinical Individual Susceptibility to Drug-Induced QT Prolongation in Healthy Subjects Using iPSC-Derived Cardiomyocytes. *Stem Cell Rep.* **2017**, *8*, 226–234. [[CrossRef](#)]
97. Blinova, K.; Schocken, D.; Patel, D.; Daluwatte, C.; Vicente, J.; Wu, J.C.; Strauss, D.G. Clinical Trial in a Dish: Personalized Stem Cell-Derived Cardiomyocyte Assay Compared With Clinical Trial Results for Two QT -Prolonging Drugs. *Clin. Transl. Sci.* **2019**, *12*, 687–697. [[CrossRef](#)]
98. Volpato, V.; Webber, C. Addressing variability in iPSC-derived models of human disease: Guidelines to promote reproducibility. *Dis. Model. Mech.* **2020**, *13*, dmm042317. [[CrossRef](#)]
99. Veerman, C.C.; Mengarelli, I.; Guan, K.; Stauske, M.; Barc, J.; Tan, H.L.; Wilde, A.A.M.; Verkerk, A.O.; Bezzina, C.R. hiPSC-derived cardiomyocytes from Brugada Syndrome patients without identified mutations do not exhibit clear cellular electrophysiological abnormalities. *Sci. Rep.* **2016**, *6*, 30967. [[CrossRef](#)]

100. Kerr, C.; Richards, D.; Menick, D.; Deleon-Pennell, K.; Mei, Y. Multicellular Human Cardiac Organoids Transcriptomically Model Distinct Tissue-Level Features of Adult Myocardium. *Int. J. Mol. Sci.* **2021**, *22*, 8482. [[CrossRef](#)]
101. Feng, W.; Schriever, H.; Jiang, S.; Bais, A.; Wu, H.; Kostka, D.; Li, G. Computational profiling of hiPSC-derived heart organoids reveals chamber defects associated with NKX2-5 deficiency. *Commun. Biol.* **2022**, *5*, 399. [[CrossRef](#)]
102. Egashira, T.; Yuasa, S.; Suzuki, T.; Aizawa, Y.; Yamakawa, H.; Matsushashi, T.; Ohno, Y.; Tohyama, S.; Okata, S.; Seki, T.; et al. Disease characterization using LQTS-specific induced pluripotent stem cells. *Cardiovasc. Res.* **2012**, *95*, 419–429. [[CrossRef](#)]
103. Ma, D.; Wei, H.; Lu, J.; Huang, D.; Liu, Z.; Loh, L.J.; Islam, O.; Liew, R.; Shim, W.; Cook, S.A. Characterization of a novel KCNQ1 mutation for type 1 long QT syndrome and assessment of the therapeutic potential of a novel IKs activator using patient-specific induced pluripotent stem cell-derived cardiomyocytes. *Stem. Cell Res. Ther.* **2015**, *6*, 39. [[CrossRef](#)]
104. Sala, L.; Yu, Z.; Ward-van Oostwaard, D.; van Veldhoven, J.P.; Moretti, A.; Laugwitz, K.L.; Mummery, C.L.; AP, I.J.; Bellin, M. A new hERG allosteric modulator rescues genetic and drug-induced long-QT syndrome phenotypes in cardiomyocytes from isogenic pairs of patient induced pluripotent stem cells. *EMBO Mol. Med.* **2016**, *8*, 1065–1081. [[CrossRef](#)]
105. Itzhaki, I.; Maizels, L.; Huber, I.; Zwi-Dantsis, L.; Caspi, O.; Winterstern, A.; Feldman, O.; Gepstein, A.; Arbel, G.; Hammerman, H.; et al. Modelling the long QT syndrome with induced pluripotent stem cells. *Nature* **2011**, *471*, 225–229. [[CrossRef](#)]
106. Lahti, A.L.; Kujala, V.J.; Chapman, H.; Koivisto, A.P.; Pekkanen-Mattila, M.; Kerkela, E.; Hyttinen, J.; Kontula, K.; Swan, H.; Conklin, B.R.; et al. Model for long QT syndrome type 2 using human iPS cells demonstrates arrhythmogenic characteristics in cell culture. *Dis. Model. Mech.* **2012**, *5*, 220–230. [[CrossRef](#)]
107. Terrenoire, C.; Wang, K.; Tung, K.W.; Chung, W.K.; Pass, R.H.; Lu, J.T.; Jean, J.C.; Omari, A.; Sampson, K.J.; Kotton, D.N.; et al. Induced pluripotent stem cells used to reveal drug actions in a long QT syndrome family with complex genetics. *J. Gen. Physiol.* **2013**, *141*, 61–72. [[CrossRef](#)]
108. Ma, D.; Wei, H.; Zhao, Y.; Lu, J.; Li, G.; Sahib, N.B.; Tan, T.H.; Wong, K.Y.; Shim, W.; Wong, P.; et al. Modeling type 3 long QT syndrome with cardiomyocytes derived from patient-specific induced pluripotent stem cells. *Int. J. Cardiol.* **2013**, *168*, 5277–5286. [[CrossRef](#)]
109. Fatima, A.; Kaifeng, S.; Dittmann, S.; Xu, G.; Gupta, M.K.; Linke, M.; Zechner, U.; Nguemo, F.; Milting, H.; Farr, M.; et al. The disease-specific phenotype in cardiomyocytes derived from induced pluripotent stem cells of two long QT syndrome type 3 patients. *PLoS ONE* **2013**, *8*, e83005. [[CrossRef](#)]
110. Malan, D.; Zhang, M.; Stallmeyer, B.; Muller, J.; Fleischmann, B.K.; Schulze-Bahr, E.; Sasse, P.; Greber, B. Human iPS cell model of type 3 long QT syndrome recapitulates drug-based phenotype correction. *Basic Res. Cardiol.* **2016**, *111*, 14. [[CrossRef](#)]
111. Kuroda, Y.; Yuasa, S.; Watanabe, Y.; Ito, S.; Egashira, T.; Seki, T.; Hattori, T.; Ohno, S.; Kodaira, M.; Suzuki, T.; et al. Flecainide ameliorates arrhythmogenicity through NCX flux in Andersen-Tawil syndrome-iPS cell-derived cardiomyocytes. *Biochem. Biophys. Rep.* **2017**, *9*, 245–256. [[CrossRef](#)]
112. Yazawa, M.; Dolmetsch, R.E. Modeling Timothy syndrome with iPS cells. *J. Cardiovasc. Transl. Res.* **2013**, *6*, 1–9. [[CrossRef](#)] [[PubMed](#)]
113. Rocchetti, M.; Sala, L.; Dreizehnter, L.; Crotti, L.; Sinnecker, D.; Mura, M.; Pane, L.S.; Altomare, C.; Torre, E.; Mostacciolo, G.; et al. Elucidating arrhythmogenic mechanisms of long-QT syndrome CALM1-F142L mutation in patient-specific induced pluripotent stem cell-derived cardiomyocytes. *Cardiovasc. Res.* **2017**, *113*, 531–541. [[CrossRef](#)] [[PubMed](#)]
114. Yamamoto, Y.; Makiyama, T.; Harita, T.; Sasaki, K.; Wuriyanghai, Y.; Hayano, M.; Nishiuchi, S.; Kohjitani, H.; Hirose, S.; Chen, J.; et al. Allele-specific ablation rescues electrophysiological abnormalities in a human iPS cell model of long-QT syndrome with a CALM2 mutation. *Hum. Mol. Genet.* **2017**, *26*, 1670–1677. [[CrossRef](#)] [[PubMed](#)]
115. Limpitkul, W.B.; Dick, I.E.; Tester, D.J.; Boczek, N.J.; Limphong, P.; Yang, W.; Choi, M.H.; Babich, J.; DiSilvestre, D.; Kanter, R.J.; et al. A Precision Medicine Approach to the Rescue of Function on Malignant Calmodulinopathic Long-QT Syndrome. *Circ. Res.* **2017**, *120*, 39–48. [[CrossRef](#)] [[PubMed](#)]
116. Cerrone, M.; Lin, X.; Zhang, M.; Agullo-Pascual, E.; Pfenniger, A.; Chkourko Guskys, H.; Novelli, V.; Kim, C.; Tirasawadichai, T.; Judge, D.P.; et al. Missense mutations in plakophilin-2 cause sodium current deficit and associate with a Brugada syndrome phenotype. *Circulation* **2014**, *129*, 1092–1103. [[CrossRef](#)]
117. Belbachir, N.; Portero, V.; Al Sayed, Z.R.; Gourraud, J.B.; Dilasser, F.; Jesel, L.; Guo, H.; Wu, H.; Gaborit, N.; Guilluy, C.; et al. RRAD mutation causes electrical and cytoskeletal defects in cardiomyocytes derived from a familial case of Brugada syndrome. *Eur Heart J.* **2019**, *40*, 3081–3094. [[CrossRef](#)]
118. Kosmidis, G.; Veerman, C.C.; Casini, S.; Verkerk, A.O.; van de Pas, S.; Bellin, M.; Wilde, A.A.; Mummery, C.L.; Bezzina, C.R. Readthrough-Promoting Drugs Gentamicin and PTC124 Fail to Rescue Nav1.5 Function of Human-Induced Pluripotent Stem Cell-Derived Cardiomyocytes Carrying Nonsense Mutations in the Sodium Channel Gene SCN5A. *Circ. Arrhythm Electrophysiol.* **2016**, *9*, e004227. [[CrossRef](#)]
119. Ma, D.; Liu, Z.; Loh, L.J.; Zhao, Y.; Li, G.; Liew, R.; Islam, O.; Wu, J.; Chung, Y.Y.; Teo, W.S.; et al. Identification of an I(Na)-dependent and I(to)-mediated proarrhythmic mechanism in cardiomyocytes derived from pluripotent stem cells of a Brugada syndrome patient. *Sci. Rep.* **2018**, *8*, 11246. [[CrossRef](#)]
120. Selga, E.; Sendfeld, F.; Martinez-Moreno, R.; Medine, C.N.; Tura-Ceide, O.; Wilmut, S.I.; Perez, G.J.; Scornik, F.S.; Brugada, R.; Mills, N.L. Sodium channel current loss of function in induced pluripotent stem cell-derived cardiomyocytes from a Brugada syndrome patient. *J. Mol. Cell Cardiol.* **2018**, *114*, 10–19. [[CrossRef](#)]

121. de la Roche, J.; Angsutararux, P.; Kempf, H.; Janan, M.; Bolesani, E.; Thiemann, S.; Wojciechowski, D.; Coffee, M.; Franke, A.; Schwanke, K.; et al. Comparing human iPSC-cardiomyocytes versus HEK293T cells unveils disease-causing effects of Brugada mutation A735V of Na(V)1.5 sodium channels. *Sci Rep.* **2019**, *9*, 11173. [[CrossRef](#)] [[PubMed](#)]
122. Jung, C.B.; Moretti, A.; Mederos y Schnitzler, M.; Iop, L.; Storch, U.; Bellin, M.; Dorn, T.; Ruppenthal, S.; Pfeiffer, S.; Goedel, A.; et al. Dantrolene rescues arrhythmogenic RYR2 defect in a patient-specific stem cell model of catecholaminergic polymorphic ventricular tachycardia. *EMBO Med.* **2012**, *4*, 180–191. [[CrossRef](#)]
123. Itzhaki, I.; Maizels, L.; Huber, I.; Gepstein, A.; Arbel, G.; Caspi, O.; Miller, L.; Belhassen, B.; Nof, E.; Glikson, M.; et al. Modeling of catecholaminergic polymorphic ventricular tachycardia with patient-specific human-induced pluripotent stem cells. *J. Am. Coll Cardiol.* **2012**, *60*, 990–1000. [[CrossRef](#)] [[PubMed](#)]
124. Preininger, M.K.; Jha, R.; Maxwell, J.T.; Wu, Q.; Singh, M.; Wang, B.; Dalal, A.; McEachin, Z.T.; Rossoll, W.; Hales, C.M.; et al. A human pluripotent stem cell model of catecholaminergic polymorphic ventricular tachycardia recapitulates patient-specific drug responses. *Dis Model. Mech* **2016**, *9*, 927–939. [[CrossRef](#)] [[PubMed](#)]
125. Sasaki, K.; Makiyama, T.; Yoshida, Y.; Wuriyanghai, Y.; Kamakura, T.; Nishiuchi, S.; Hayano, M.; Harita, T.; Yamamoto, Y.; Kohjitani, H.; et al. Patient-Specific Human Induced Pluripotent Stem Cell Model Assessed with Electrical Pacing Validates S107 as a Potential Therapeutic Agent for Catecholaminergic Polymorphic Ventricular Tachycardia. *PLoS ONE* **2016**, *11*, e0164795. [[CrossRef](#)]
126. Novak, A.; Barad, L.; Lorber, A.; Gherghiceanu, M.; Reiter, I.; Eisen, B.; Eldor, L.; Itskovitz-Eldor, J.; Eldar, M.; Arad, M.; et al. Functional abnormalities in iPSC-derived cardiomyocytes generated from CPVT1 and CPVT2 patients carrying ryanodine or calsequestrin mutations. *J. Cell Mol. Med.* **2015**, *19*, 2006–2018. [[CrossRef](#)]
127. Maizels, L.; Huber, I.; Arbel, G.; Tijssen, A.J.; Gepstein, A.; Khoury, A.; Gepstein, L. Patient-Specific Drug Screening Using a Human Induced Pluripotent Stem Cell Model of Catecholaminergic Polymorphic Ventricular Tachycardia Type 2. *Circ. Arrhythm Electrophysiol.* **2017**, *10*, e004725. [[CrossRef](#)]
128. Kim, C.; Wong, J.; Wen, J.; Wang, S.; Wang, C.; Spiering, S.; Kan, N.G.; Forcales, S.; Puri, P.L.; Leone, T.C.; et al. Studying arrhythmogenic right ventricular dysplasia with patient-specific iPSCs. *Nature* **2013**, *494*, 105–110. [[CrossRef](#)]

Disclaimer/Publisher’s Note: The statements, opinions and data contained in all publications are solely those of the individual author(s) and contributor(s) and not of MDPI and/or the editor(s). MDPI and/or the editor(s) disclaim responsibility for any injury to people or property resulting from any ideas, methods, instructions or products referred to in the content.